ANALYSIS OF DEVONIAN SHALE MULTI-WELL INTERFERENCE TESTS IN MEIGS COUNTY, OHIO

Final Report

February 23, 1982

Contributing Authors: J. Alam, K. Horan, B. Lee, W. Sawyer

Prepared for:
Morgantown Energy Technology Center
U.S. Department of Energy
P.O. Box 880
Morgantown, WV 26505

Prepared by:
Science Applications, Inc.
Suite 8, Chestnut Ridge Professional Building
Morgantown, WV 26505

Prepared under Contract #DE-AC21-81MC16283

"This report was prepared as an account of work sponsored by an agency of the United States Government. Neither the United States Government nor any agency thereof, nor any of their employees, makes any warranty, express or implied, or assumes any legal liability or responsibility for the accuracy, completeness, or usefulness of any information, apparatus, product, or process disclosed, or represents that its use would not infringe privately owned rights. Reference herein to any specific commercial product, process, or service by trade name, trademark, manufacturer, or otherwise, does not necessarily constitute or imply its endorsement, recommendation, or favoring by the United States Government or any agency thereof. The views and opinions of authors expressed herein do not necessarily state or reflect those of the United States Government or any agency thereof."

EXECUTIVE SUMMARY

EXECUTIVE SUMMARY

The Offset Well Test Program completed in 1981 was undertaken in order to investigate the production characteristics of Devonian shale reservoirs. The investigation involved a study of gas flow through natural fractures, the orientation and distribution of these fractures, and the gas storage/release mechanism and its effect on production. An experiment was designed to test the reservoir under strictly controlled conditions. Interference tests were conducted on two wells drilled in the expected maximum and minimum permeability directions from a producing well with known completion and production history.

Columbia Gas Well 10056 in Meigs County, Ohio, in the Appalachian Basin, was chosen as the test site. Targeted for the Lower Huron, 450 feet of core was retrieved from offset well 10056A. In the Initial testing, a series of build-ups (short-term interval tests-STT), was conducted, followed by a longer period of interference testing (long-term tests, LTT). This included buildup in the offset wells to stabilization, followed by shutting in the central (control well), and observing interference response in the offset wells. The control well was then flowed at constant backpressure, and response was monitored in the offset wells. These tests were followed by a series of pulse tests, which included a 24-hour buildup period of the control well followed by a 24-hour flow at constant pressure. Upon completion of the pulse tests, far field interference was investigated by observing the response in nearby wells. Field activities were completed during August 1981.

Analysis of the test results indicate that the Devonian shale formation in the Meigs County, Ohio, area is an anisotropic, layered reservoir system. Flow characteristics indicate that the Meigs County reservoir is naturally fractured, may be represented as a dual porosity system, and may be modeled using pseudo-steady-state gas transfer from the matrix to the fracture system. The orientation of the natural fracture system was established through core observation and well test analysis as S65^{o}W. The maximum to minimum permeability ratio in the direction of the natural fracture system was calculated to be 8.3. Three distinct zones with independent flow characteristics were identified. The bottom zone, with permeability values significantly higher than the upper two zones, is highly fractured and is a

1.0

INTRODUCTION AND BACKGROUND

1.0 INTRODUCTION AND BACKGROUND

1.1 Eastern Gas Shales Project/Offset Well Test Program Goals

A multi-well test program was established in 1979 as a part of the U.S. Department of Energy's Eastern Gas Shales Project (EGSP) with the overall objective of defining the production characteristics of naturally fractured eastern Devonian shale gas reservoirs. The program designated as the Offset Well Test Program (OWTP) was undertaken in order to investigate the following Devonian shale reservoir parameters:

- Flow characteristics of gas in fractured shale
- Orientation and distribution of natural fractures
- Storage and release mechanisms of gas from the shale
- Directional gas flow and impact on production practices

The Offset Well Test Program plan included the drilling of two offset observation wells in the directions of expected maximum and minimum permeability trends from a central producing well with a recorded production history. A series of tests designed for the offset wells included short-term interval testing, interference testing, pulse testing, and far-field interference testing. During the testing phase, the central producing (control) well was to be operated under closely controlled conditions of constant pressure, and pressure measurements as a function of time were to be made in the observation wells.

This closely monitored experiment was designed to provide data on in situ permeabilities and porosities that can be directly correlated to the in situ fracture system, and to yield specific information on the reservoir's anisotropy and heterogeneity. Test results, when analyzed, define reservoir production mechanisms, a knowledge of which helps to improve stimulation treatments, optimize well spacing, and determine the quantity of producible Devonian shale gas.

S55^{o}E direction. This completed Phase II of the project. Figure 3 is a schematic of the well locations at surface and bottom hole showing deviation of the wellbores with depth.

The core retrieved from Well 10056A was handled by Cliffs Minerals, Inc., and SAI using standard EGSP procedures. It was distributed to the following organizations for specific analyses:

- Core Labs: matrix porosity, matrix permeability, Klinkenberg factor
- Battelle Columbus Laboratories: offgassing, reservoir model validation, storage mechanisms, porosity, permeability, Klinkenberg factor
- SAI and Halliburton: mechanical tests for stimulation design
- Mound Laboratory: gas sampling, bulk density, permeability

A dry-hole suite of logs consisting of gamma-ray, neutron, density, caliper, induction, temperature, and audio was run in both wells. A gas show was evident between 3,378 and 3,392 feet in Well 10056A. Temperature logs run on both wells later in March prior to testing indicated gas entry at the same bottom zone.

- Phase III: Testing

Testing began in March 1981 with 17 days of six short-term tests run on both offset wells. The purpose of these tests was to provide wellbore pressure profiles and a means for identifying the shale zones in communication with the wellbores. Figures 4 and 5 show the pressure levels, the duration of each short-term test, and well logs for Wells 10056A and 10056B, respectively. These tests were to identify the three zones for interference testing, which are as follows:

<u>10056A</u>

Zone 1 - 3,324 to 3,405 feet (81 feet)

Zone 2 - 3,248 to 3,319 feet (71 feet)

Zone 3 - 3,177 to 3,243 feet (66 feet)

<u>10056B</u>

Zone 1 - 3,329 to 3,410 feet (81 feet)

Zone 2 - 3,253 to 3,324 feet (71 feet)

Zone 3 - 3,182 to 3,248 feet (66 feet)

2.0

WELL TEST ANALYSIS - ANALYTICAL STUDY

Long-term interference testing began on March 29, 1981 with pre-long-term testing, in which both offset wells were shut in to allow pressures to stabilize in wellbores and reservoir. On April 20, the control well was shut in for the pressure buildup phase of interference testing. This phase continued for 50 days, two weeks of which were spent in pulling and resetting the packers and restabilizing the wellbore pressures due to packer blowout. The drawdown phase of interference testing began on June 9 and continued for 38 days. Constant wellhead pressure was maintained at the control well during drawdown.

Long-term interference test pressure profiles are shown in Figures 6 and 7 for offset wells 10056A and 10056B, respectively.

A series of short-duration pulse tests was next conducted to help identify and quantify shale fracture properties while eliminating long-term matrix effects. In three series of pulse tests, the control well was shut in for 24 hours and opened for the following 24 hours, flowing at constant pressure. All zones in both offset wells, with the exception of the top zone in Well 10056B, responded to the pulse.

Far-field interference testing was conducted in order to determine the extent of communication between the test area wells. Three neighboring producing wells between 1700 to 3500 feet from the test site (Wells No. 9974, 8242, and 9553), were shut in on July 27, 1981. Fourteen days of far-field interference testing detected no measurable response in either offset well.

The shutdown of field operations was initiated on August 10, 1981. The service rig was set up on each offset well, measuring flow rates by zone. Packers and downhole instruments were removed from the offset wells and the pressure probe retrieved from the control well. All equipment was removed from the site on September 17, 1981. Phase III was completed September 30, 1981 with the submittal of the final report on field activities.

- Phase IV: Well Test Analysis

The project test data is analyzed in this report, submittal of which completes Phase IV of the Offset Well Test Program and all planned activities under the program. The analysis is presented in two identifiable approaches:

- Analytical Method
- Numerical Method

Each approach is discussed independently. Conclusions and recommendations are based on the combined results of both approaches.

2.0 WELL TEST ANALYSIS - ANALYTICAL STUDY

The analytical approach to well test data from the Meigs County, Ohio, test site has been divided into the following sections:

2.1 Flow Rate Calculation
2.2 Control Well Analysis
2.3 Interference Data Analysis
2.4 Pulse Test Analysis
2.5 Reservoir Anisotropy Calculations
2.6 Reservoir Drainage Volume Calculations

2.1 Flow Rate Calculation

In analyzing the Meigs County, OH, test data, it was understood that wellbore storage characteristics would affect the interference and pulse tests by causing a delay in pressure responses. Therefore, it was important to accurately determine flow rates for the various zones tested. The flow rates were also needed to calculate permeability (k_f) from type curve matches. After completion of testing, the annulus, top, middle, and total zone flow rates were measured in the field. It was determined that flow rate calculations using early well test data were sufficiently accurate for this analysis.

The equation used in this calculation is derived from the wellbore storage coefficient and the log-log unit slope line used to estimate the apparent wellbore storage coefficient.

$$C = V_w c = \frac{qB_g}{(1000)\ 24} \frac{\Delta t}{\Delta p} \qquad (1)$$

where
- C - wellbore storage coefficient (cu.ft./psi)
- V_w - total wellbore volume (cu.ft.)
- c - compressibility of the gas in the wellbore (psi^{-1})
- q - flow rate (MCFD)
- B_g - volumetric factor of gas
- Δp - pressure change during the test (psi)
- Δt - test time (hr.)

From the equation of state for real gas, it is known that

$$Bg = \frac{p_{sc}TZ}{pT_{sc}}$$

Equation (1), rearranged for the flow rate calculation, assumes that the compressibility of gas is the inverse of average pressure at the wellbore and that Z has a factor of one.

$$q(MCFD) = \frac{24T_{sc}V_w}{(1000)\ p_{sc}T}\ \frac{(\Delta p)}{(\Delta t)}$$

Total wellbore volumes for the final three zones were obtained from the Lynes instrument schematic*, as follows:

Bottom Zone: $V_w = \pi\left[\left(\frac{7-7/8}{24}\right)^2 - \left(\frac{2-3/8}{24}\right)^2\right]\ (81) = 24.91$

Middle Zone: $V_w = \pi\left[\left(\frac{7-7/8}{24}\right)^2 - \left(\frac{2-3/8}{24}\right)^2\right](71)+(2+5+71+66+5+3)\ \pi\left(\frac{2-3/8}{24}\right)^2 = 26.66$

Top Zone: $V_w = \pi\left[\left(\frac{7-7/8}{24}\right)^2 - \left(\frac{2-3/8}{24}\right)^2\right]\ (66) = 20.29$

In calculating the wellbore volume of the middle zone, the inside volume of tubing from the shut-in tool to the bottom packer was considered. The following flow rate calculations were based on the unit slope lines shown in Figures 8 through 13:

---

*A schematic of the Lynes instrumentation is presented in the "Final Report on Field Activities" by Science Applications, Inc., Sept. 30, 1981, DOE/METC Contract #DE-AM21-78MC08216, Task 23.

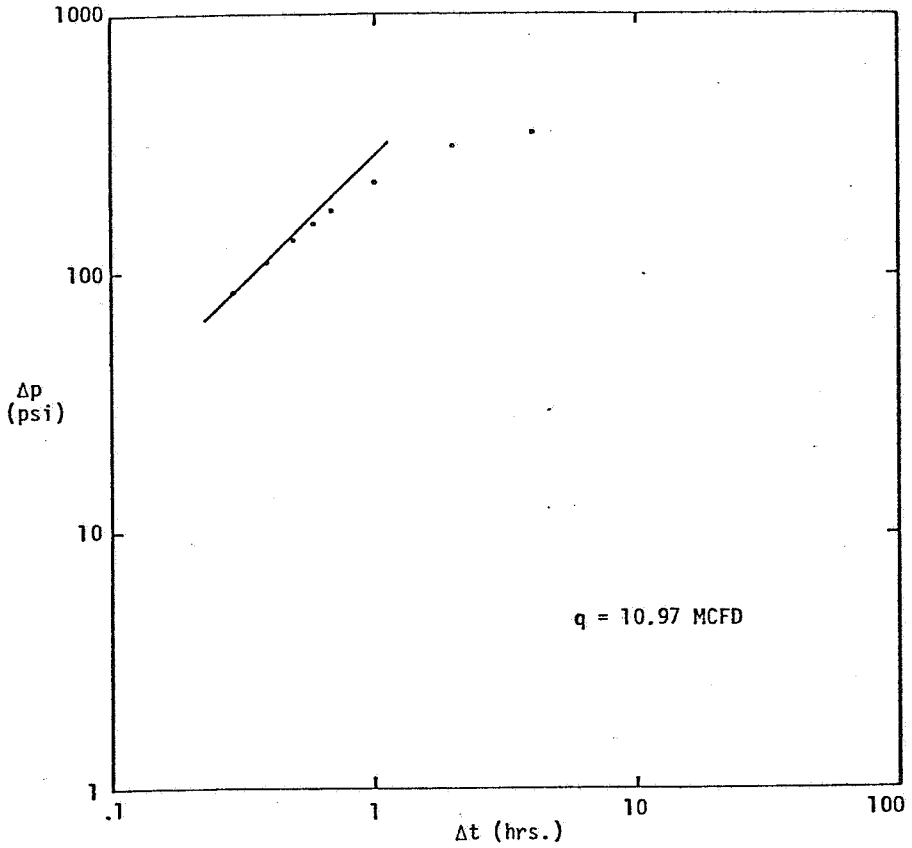

Figure 8: Log-Log Plot of Pre-Long-Term Test Buildup, Bottom Zone Well 10056A

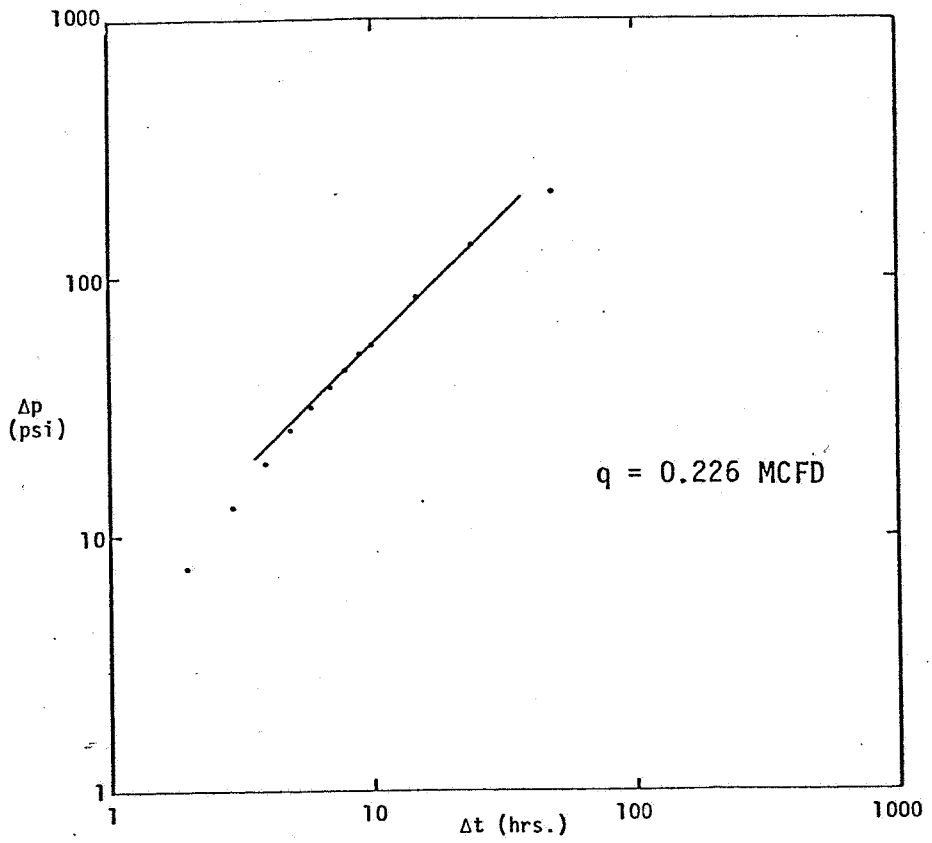

Figure 9: Log-Log Plot of Pre-Long-Term Test Buildup, Middle Zone of Well 10056A

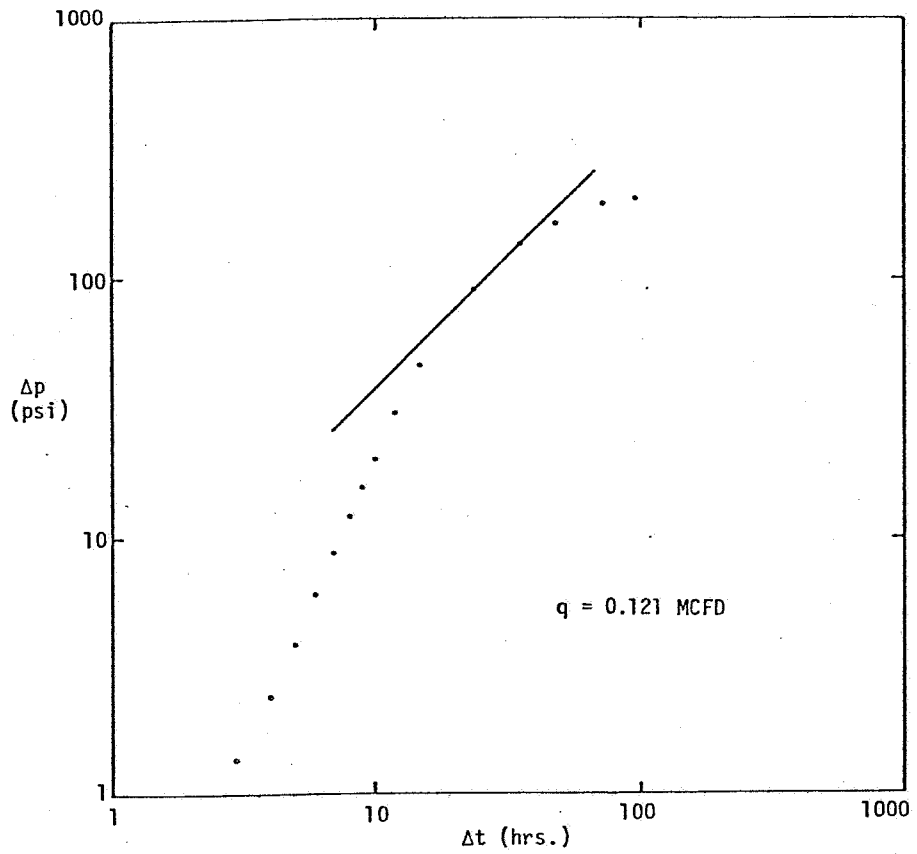

Figure 10: Log-Log Plot of Pre-Long-Term Test Buildup, Top Zone Well 10056A

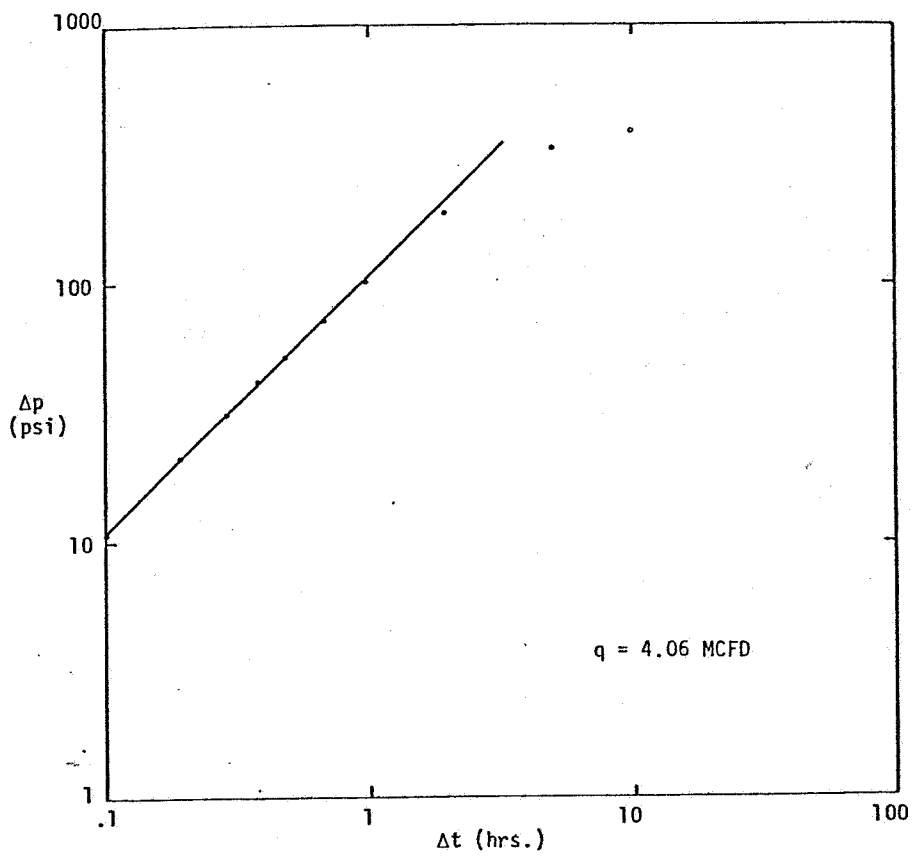

Figure 11: Log-Log Plot of Pre-Long-Term Test Buildup, Bottom Zone of Well 10056B

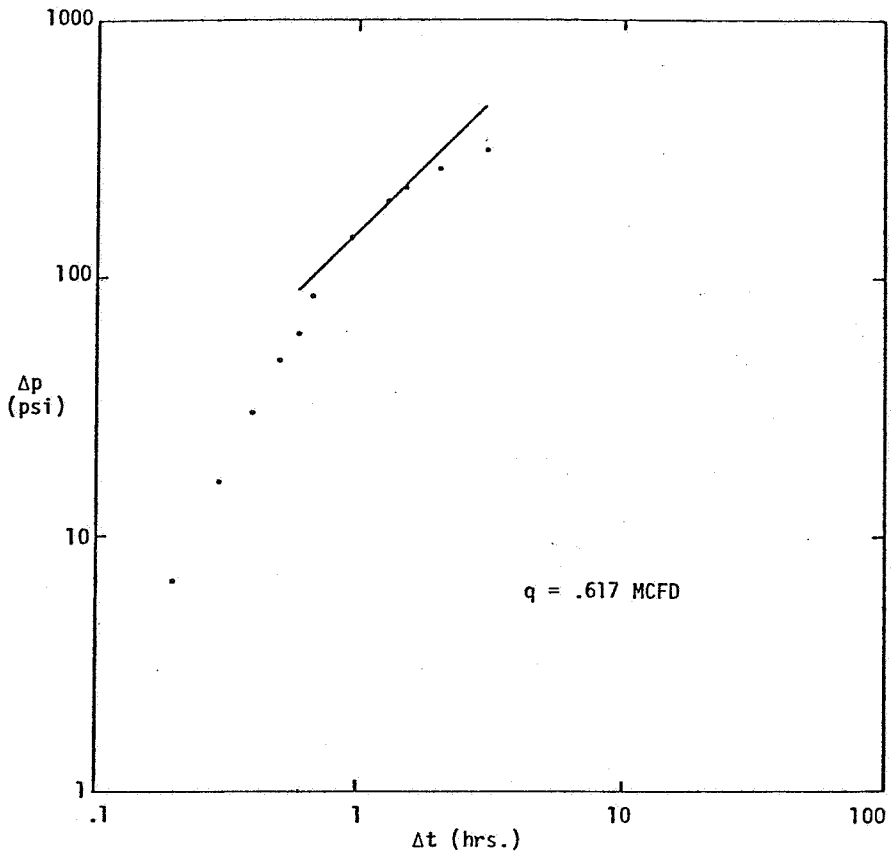

Figure 12: Log-Log Plot of Pre-Long-Term Test Buildup, Middle Zone Well 10056B

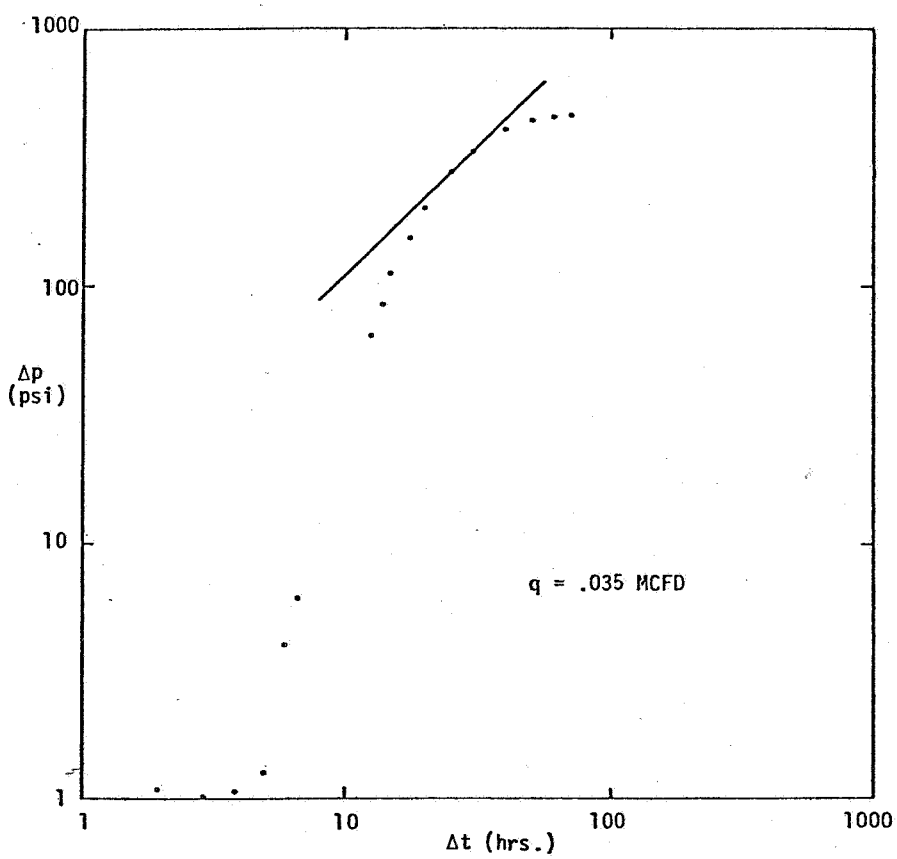

Figure 13: Log-Log Plot of Pre-Long-Term Test Buildup, Top Zone Well 10056B

$$PA1: \quad q = \frac{24x(520)x(24.91)}{1000x(14.7)x(540)} \frac{(140)}{(0.5)} = 10.97 \text{ MCFD}$$

$$PA2: \quad q = \frac{24x(520)x(26.66)}{1000x(14.7)(554)} \frac{(133)}{(24)} = 0.226 \text{ MCFD}$$

$$PA3: \quad q = \frac{24x(520)(20.29)}{1000x(14.7)(554)} \frac{(93.1)}{(24)} = 0.121 \text{ MCFD}$$

$$PB1: \quad q = \frac{24x(520)(24.91)(42)}{1000x(14.7)(547)(0.4)} = 4.06 \text{ MCFD}$$

$$PB2: \quad q = \frac{24x(520)(26.66)(223.77)}{1000x(14.7)(547)(15)} = .617 \text{ MCFD}$$

$$PB3: \quad q = \frac{24x(520)(20.29)(333)}{1000x(14.7)(547)(300)} = .035 \text{ MCFD}$$

These results shown in Table 1 are close to actual measurements.

Considering the possibility of error inherent in changing the orifice plates and reading the gauge, flow rate calculations based on early-time well test data are judged to be very accurate.

Using the same equation, the flow rate for the control well was calculated. It was also obtained from the meter connected to the pipeline and from well records. The log-log graph for the control well (Figure 14) shows a flow rate of 19 MCFD, which is identical to daily measurements made at the pipeline gauge, and results from the simulator. The flow rate of 19 MCFD was used in this analysis.

Figures 15 through 17 present the same approaches for Well 10056A buildup data that were obtained following remedial operation for packer blow-off that occurred on May 2, 1981.

In this case, the flow rates for each zone are: q_{PA1} = 10.93 MCFD; q_{PA2} = .96 MCFD; q_{PA3} = .46 MCFD. Although the flow rates in the upper two zones are small, the calculated values are very consistent with rates obtained from the pre-long term test buildup and the actual field measurements.

The total flow rate of Well 10056A is calculated at 11.317 MCFD and Well 10056B at 4.712 MCFD. In Well 10056A, 97% of the flow comes from the bottom zone, 2% from the middle zone, and 1% from the top zone. In Well 10056B, the bottom zone contributes 86%, the middle zone 13% and the top zone 1%. In type curve analysis of the offset wells, the control well flow rate of 19 MCFD was divided by using the above percentages for each zone. For the analysis of Well 10056A, the flow rate was 18.43 MCFD from the bottom zone; .38 MCFD from the middle zone, and .19 MCFD from the top zone. For the analysis of Well 10056B, the flow rate was 16.34 for the bottom zone, 2.47 MCFD for the middle zone, and .19 MCFD for the top zone.

TABLE 1: Results of Flow Rate Measurement

WELL 10056A			
Zone	Size of Orifice Plate (inches)	Depth of Water (inches)	Flow Rate (MCFD)
Annulus	0.125	0.75	0.435
Top (PA3)	.25	1.9	2.19
Middle (PA2)	.125	1.8	.672
Bottom (PA1) (calculated) .	--	--	12.05
Total Well	.75	1.3	15.35

WELL 10056B			
Zone	Size of Orifice Plate (inches)	Depth of Water (inches)	Flow Rate (MCFD)
Annulus	0.125	0.3	0.275
Top (PB3)	--	--	T.S.M.* (0.05)
Middle (PB2)	.125	.7	.42
Bottom (PA1) (calculated) .	--	--	4.01
Total Well	.375	1.95	4.755

*T.S.M.: Too small to measure

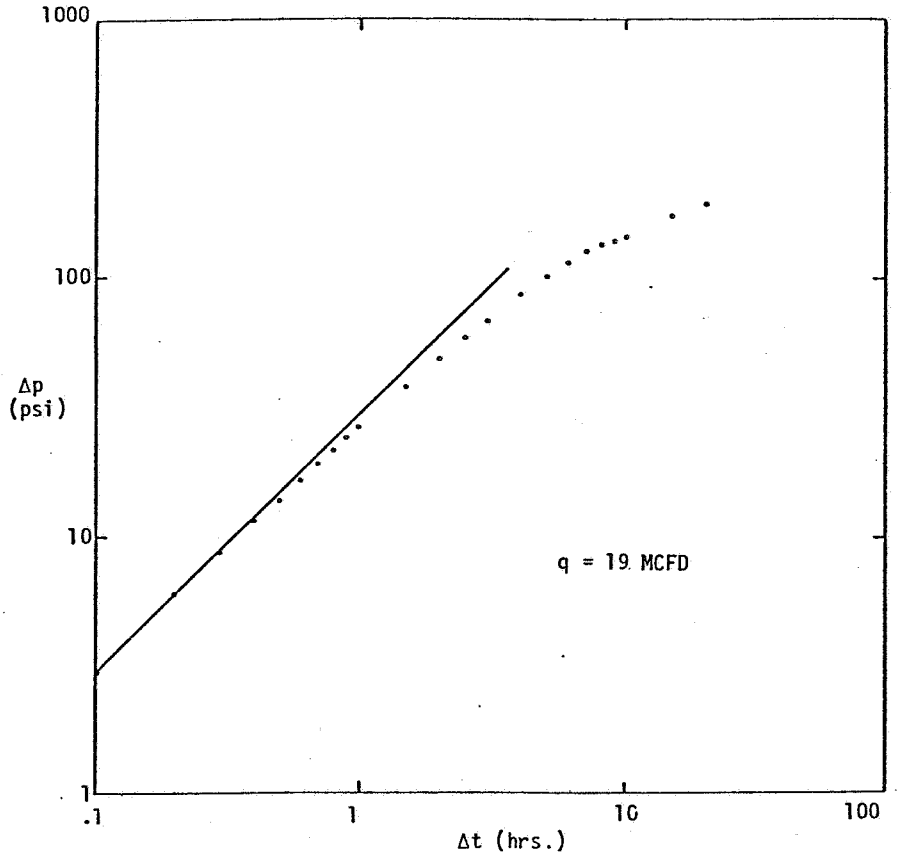

Figure 14: Log-Log Plot of Control Well Buildup During the Pre-Long-Term Testing

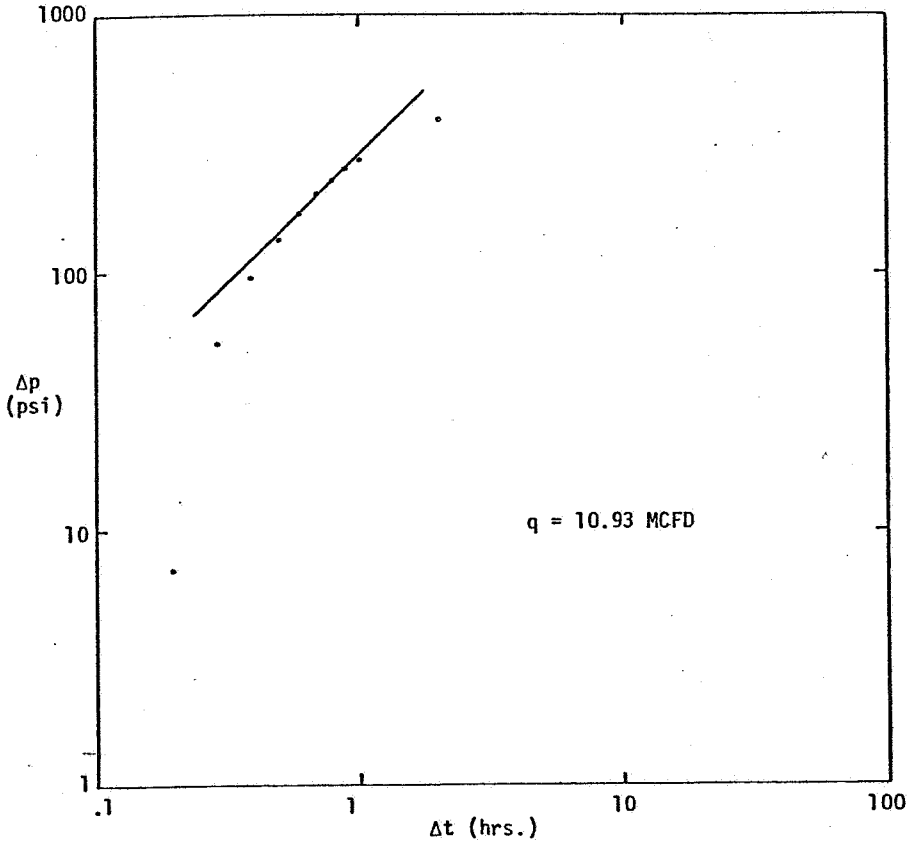

Figure 15: Log-Log Plot of Bottom Zone of Well 10056A After the 5/2/81 Packer Blowout

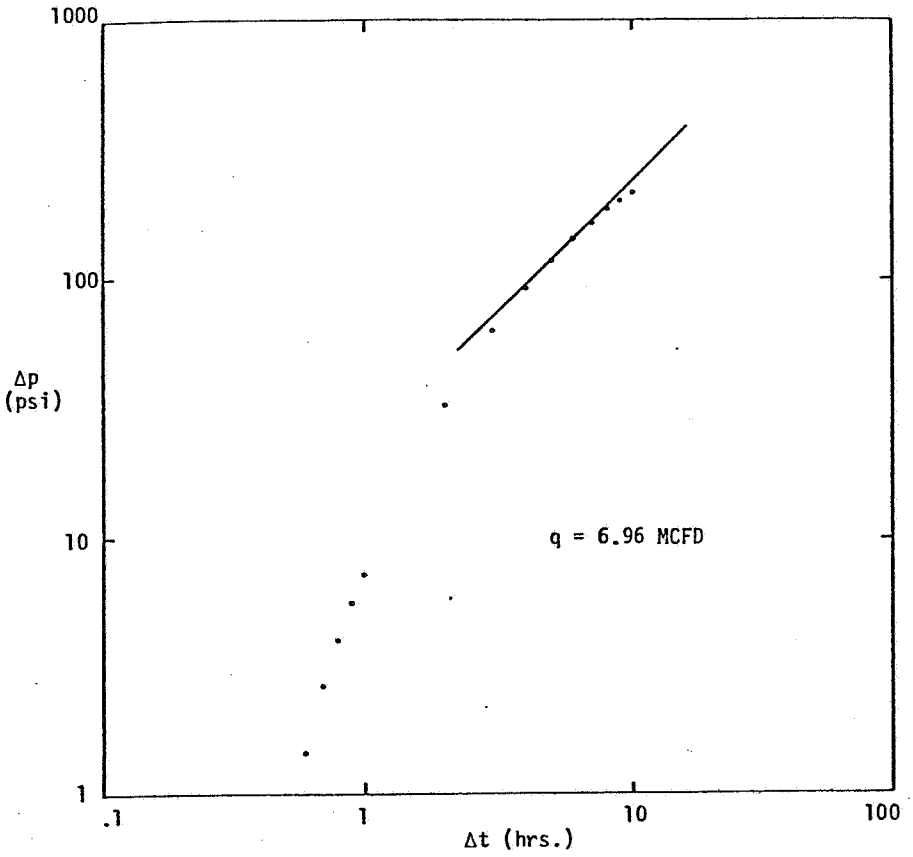

Figure 16: Log-Log Plot for Middle Zone of Well 10056A after the 5/2/81 Packer Blowout

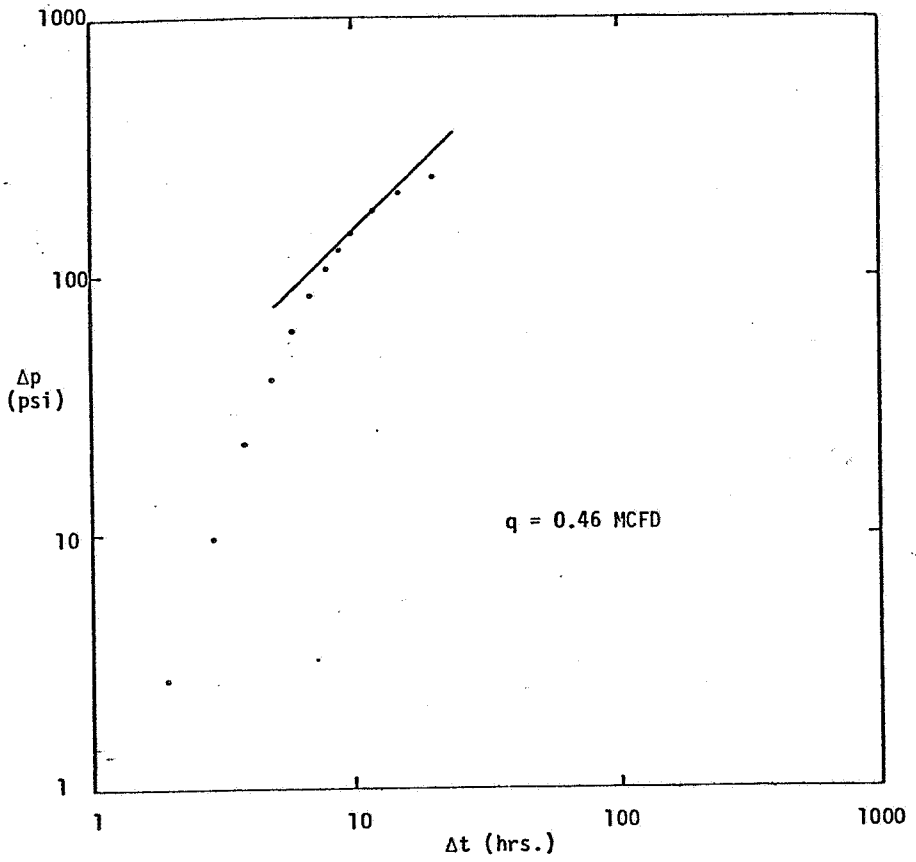

Figure 17: Log-Log Plot for Top Zone of Well 10056A After the 5/2/81 Packer Blowout

This value of C_D shows excellent agreement with the matching parameter $C_D = 10^4$. The permeability - thickness product, $k_f h$, can be recalculated from the general relationship from the type curve matching technique as follows:

$$\frac{t_D}{C_D} = \frac{0.000264\ kht\ (2\pi)}{\mu c}$$

$$3 = \frac{0.000264\ kh(10)(2\pi)}{(0.0115)(1.6)}$$

$$k_f h = 3.33 \quad \text{md-ft}$$

This calculation was used to check the accuracy of semilog and type curve analyses.

In summary, the following table is constructed from the analysis of the control well buildup data, and are believed to be average, or effective, values.

	$k_f h$ (md-ft)	$\phi_f c$ (psi^{-1})	C_D	s
Semilog	2.9	-	-	-2.6
Type Curve	3.107	1.8×10^{-6}	10^4	-2

This analysis is based on an isotropic homogeneous, single porosity, cylindrical reservoir. The type curve used for this study is presented in Figure 20.

The interference test analysis that follows is based on a dual porosity model, specifically the Warren and Root model. New type curves for a dual porosity, isotropic reservoir, with wellbore storage and skin effects were generated. Since it is assumed based on our calculations that $C_D = 10^4$ and $s = -2$, two specific type curves were generated and are presented in Figures 21 and 22. As a result of experience gained, the analysis was focused using $\omega = 0.1$ to 0.01 and $\lambda = 10^{-7}$ to 10^{-4}.

2.4 Pulse Test Analysis

The approach to pulse test analysis has been to use conventional methods, based on a single porosity, isotropic radial reservoir. Pulse testing in naturally fractured reservoirs is relatively new and the theoretical base has not been fully developed. The assumption that a naturally fractured reservoir will behave as a homogeneous reservoir during pulse testing is sound, since in naturally fractured reservoirs, early-time pressure behavior is controlled by the fracture flow mechanism. Pulse tests are based on early-time pressure behavior of the reservoir. Another aspect of pulse test analysis is that no general solutions have been published for wellbore storage and skin effects of the pulsing (control) well on pulse test response. Prats and Scott[21] reported that wellbore storage in observation wells caused the time lag to increase and the pressure amplitude to decrease. Mondragon and Menzie[22] studied an empirical method to correct the results of wellbore storage at the pulsing well. They, too, concluded that wellbore storage at the pulsing well increases the time lag and reduces the pressure amplitude, but they failed to find a correction factor or relationship for a general solution to this problem.

Based on the above considerations, Kamal and Brigham's[23] conventional general approach for the design and analysis of pulse tests is applied. It should be acknowledged that this application will result in the transmissibility (mainly k_f) being underestimated, and the storativity (mainly $\phi_f c_t$) being overestimated.

Pulse test data plots for all zones at both offset wells are presented in Figures 50 through 55. The difference of pressure squared versus time in hours is plotted. As mentioned in the previous section, PA2 and PA3 pressures (middle and top zones of Well 10056A) decreased or stayed at the same level during the pulse test, possibly due to mechanical leaks. Even though control well pressure decreased briefly during the first and second shut-in periods, pressure response at the bottom zone of Well 10056B (PB1) shows a typical, textbook-type pulse test curve. Pressure responses from the middle and top zones (PB2, PB3) of Well 10056B are marginal.

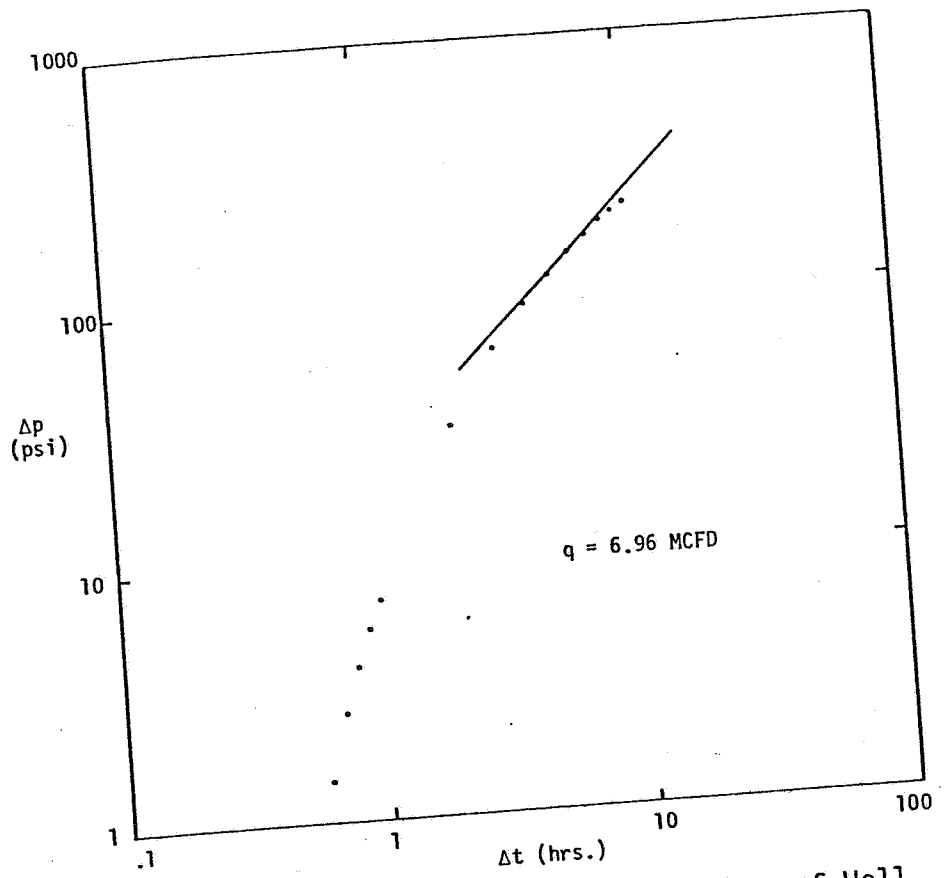

Figure 16: Log-Log Plot for Middle Zone of Well 10056A after the 5/2/81 Packer Blowout

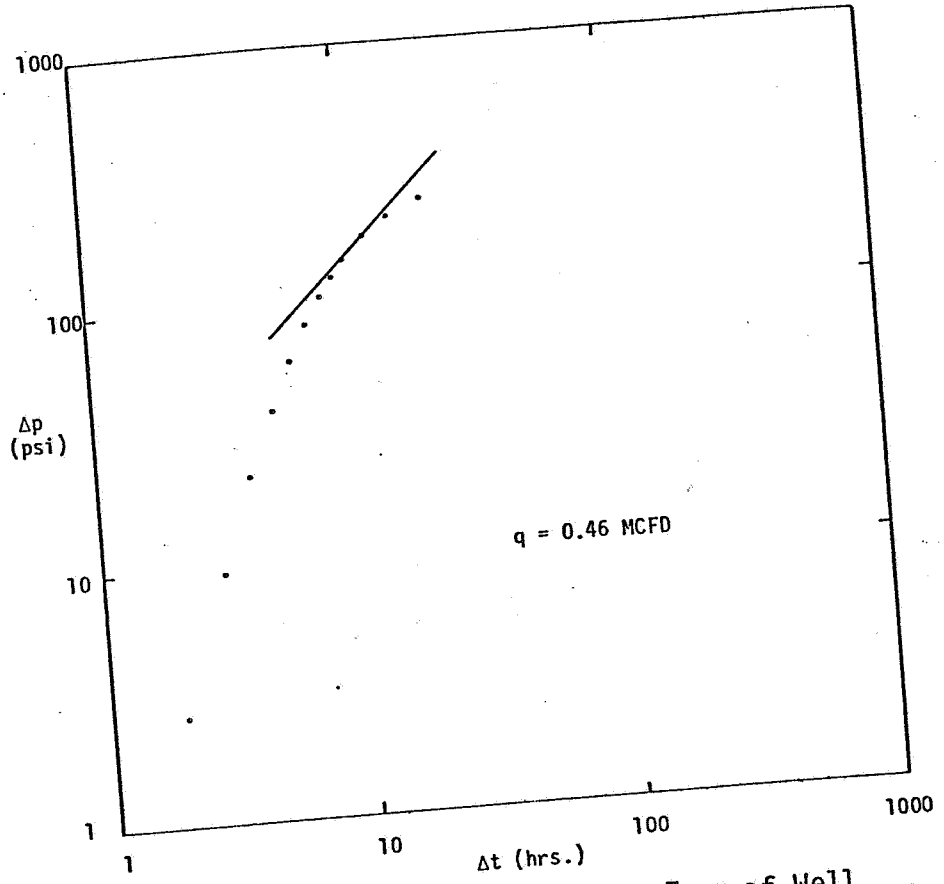

Figure 17: Log-Log Plot for Top Zone of Well 10056A After the 5/2/81 Packer Blowout

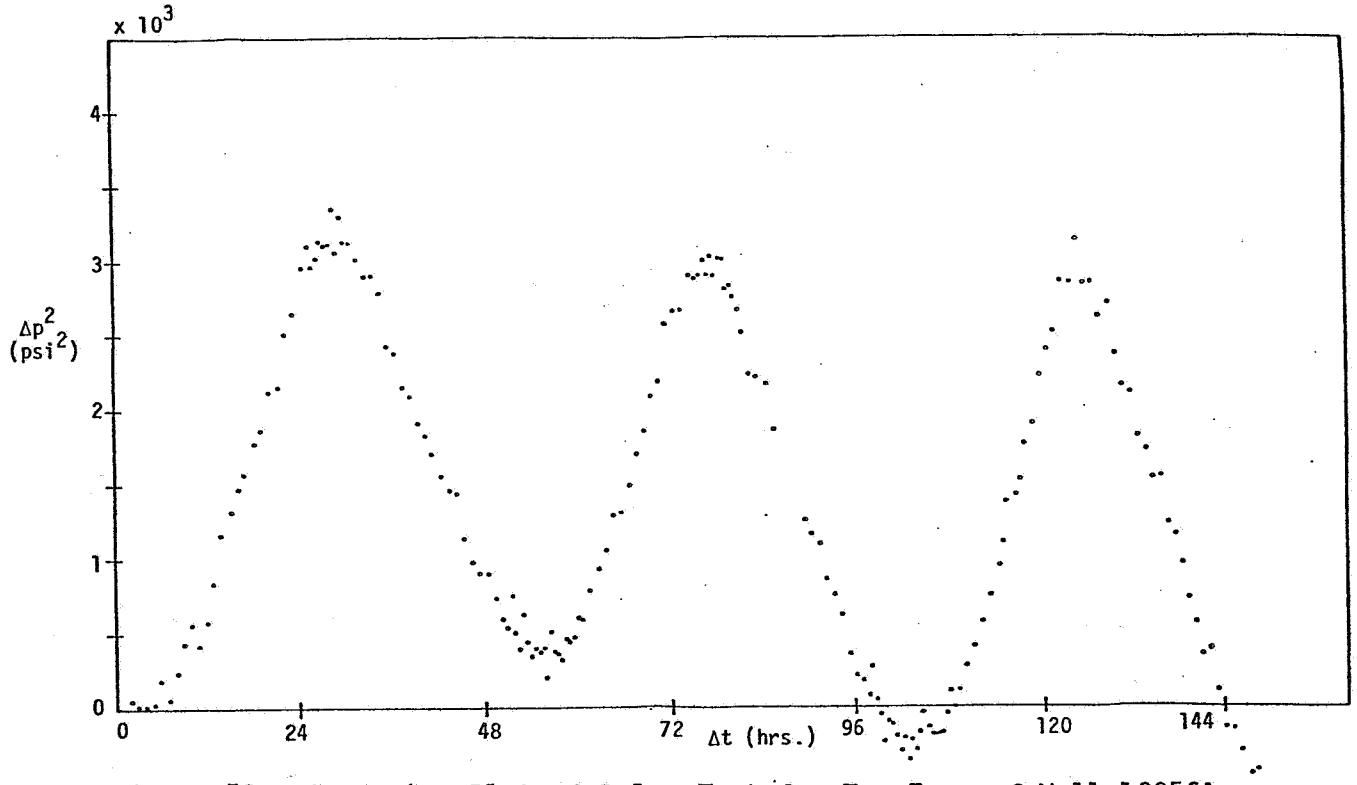

Figure 52: Cartesian Plot of Pulse Test for Top Zone of Well 10056A

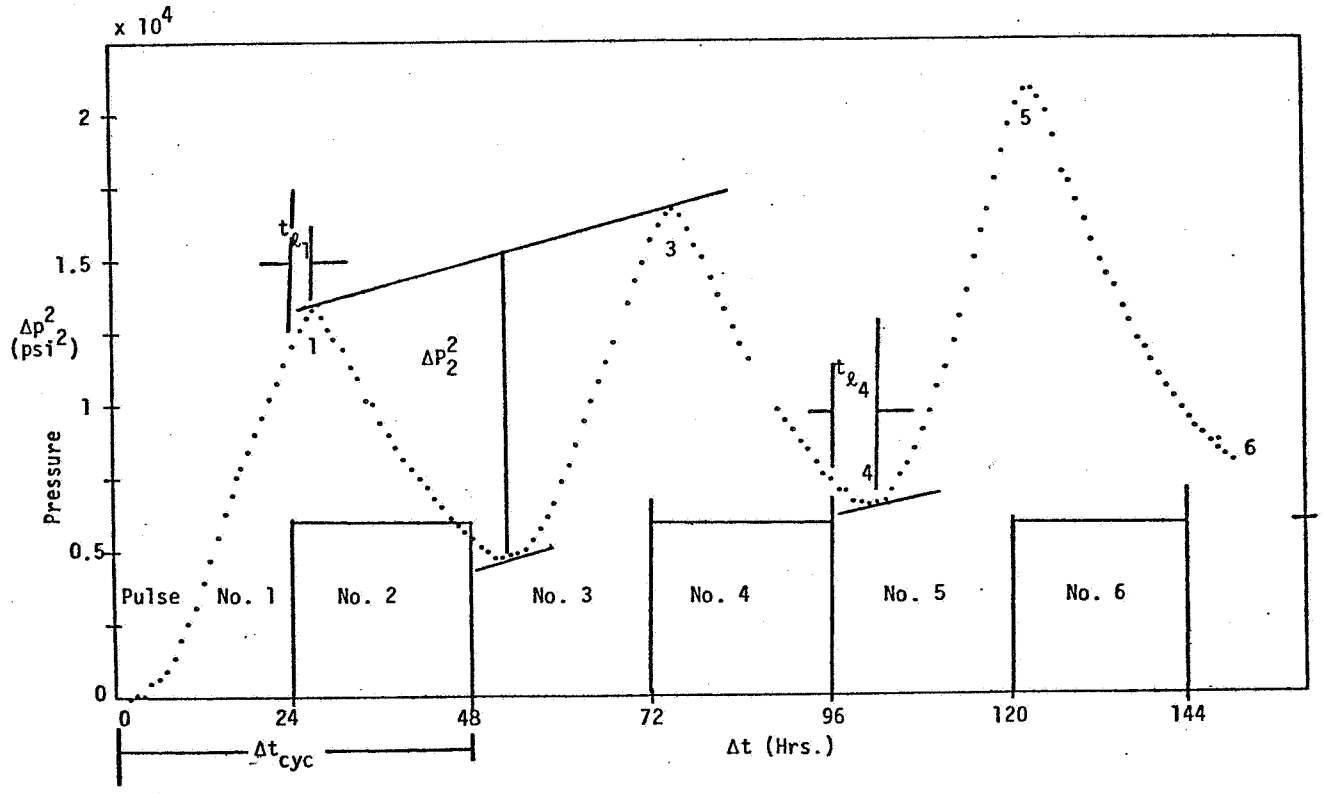

Figure 53: Cartesian Plot of Pulse Test for Bottom Zone of Well 10056B

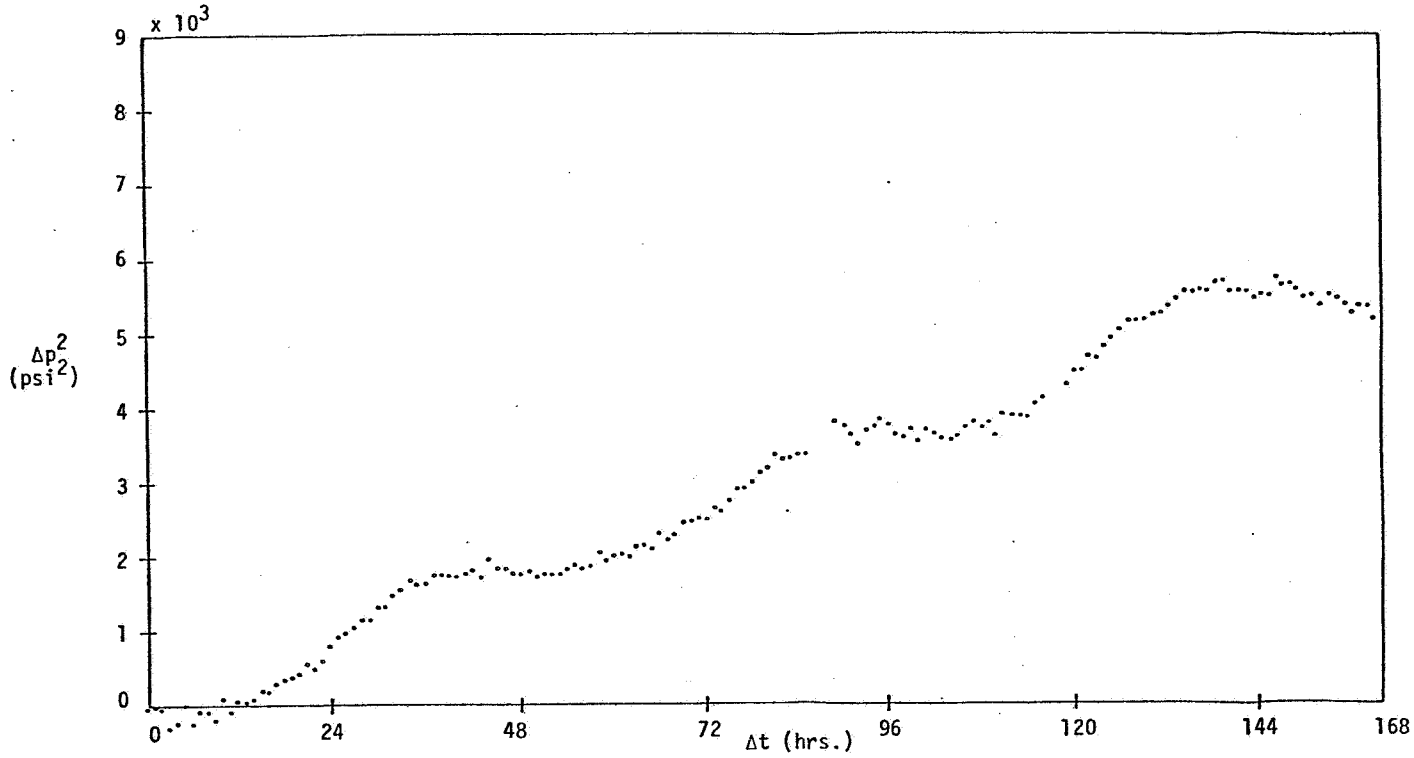

Figure 54: Cartesian Plot of Pulse Test for Middle Zone of Well 10056B

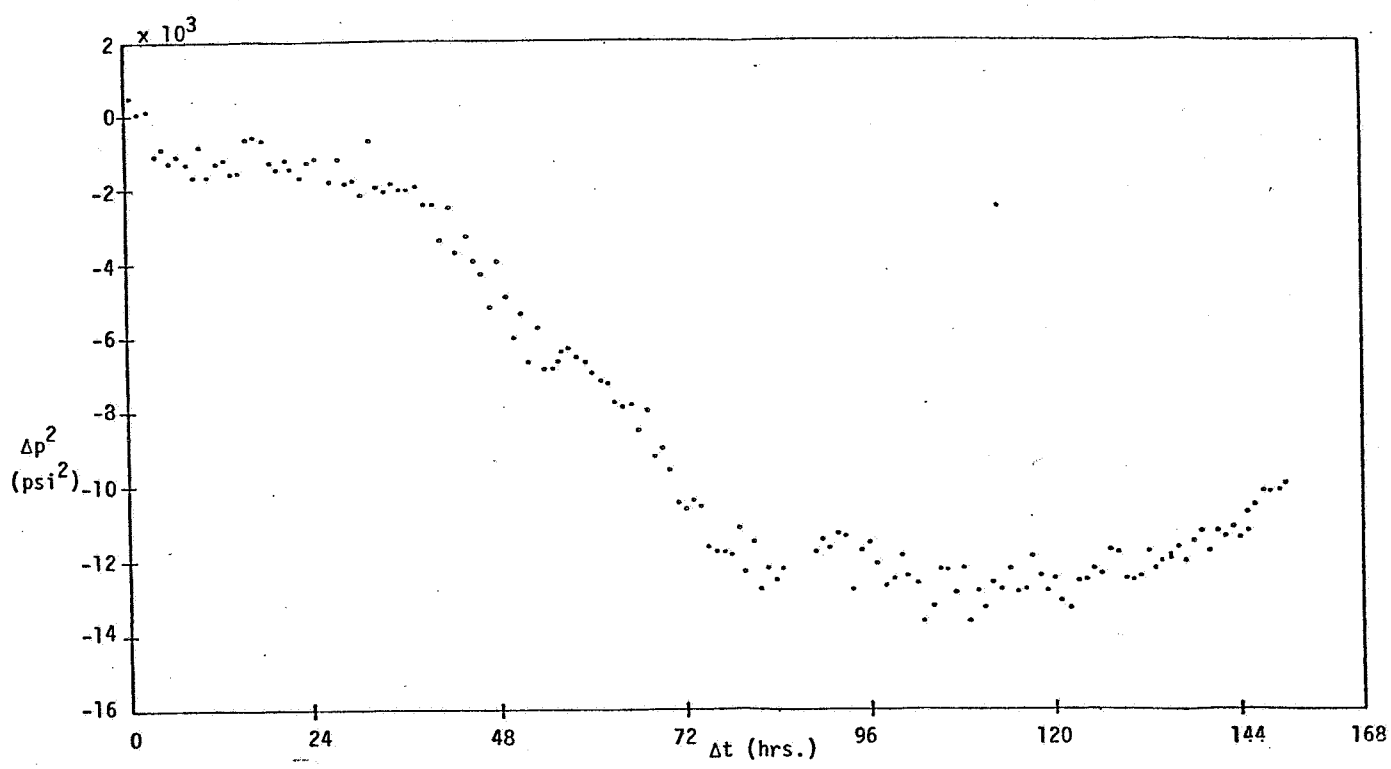

Figure 55: Cartesian Plot of Pulse Test for Top Zone of Well 10056B

As explained by Kamal and Brigham[23], the following equation relates the dimensionless cycle period to the dimensionless time lag:

$$\Delta t_{cycD} = Ct_{\ell D}^{A} + D \tag{3}$$

where D = -0.325 for odd pulses and D = -0.675 for even pulses. A and C are functions of the pulse ratio. The dimensionless parameters are defined by the following equations:

$$\Delta t_{cyc}{}^{D} = \frac{k\Delta t_{cyc}}{56{,}900\phi c_t \mu r^2} \qquad (\Delta t \text{ in minutes}) \tag{4}$$

$$t_{\ell D} = \frac{t_\ell}{\Delta t_{cyc}}$$

where, Δt_{cyc} is the cycle period (which is the sum of the pulse period and the shut-in period), and t_ℓ is the time lag. The pulse ratio is defined as pulse period divided by cycle period which, in this test, is 0.5. The following equation relates the dimensionless time lag, the dimensionless cycle period, and the dimensionless pressure response amplitude:

$$\Delta p_D/\Delta t_{cycD} = H\left[F \exp\left(Et_{\ell D}\right) + 0.01\right] \tag{5}$$

where H = -1 (odd pulses) and H= 1 (even pulses). E and F are also functions only of the pulse ratio. Dimensionless pressure in gas reservoirs is defined by:

$$\Delta p_D = \frac{kh\Delta p^2}{712\, q\mu ZT} \tag{6}$$

The coefficients for the above two equations, given by Kamal and Brigham, are presented in Table 4. The pulse ratio is 0.5 for the different odd and even pulses.

Table 4: Pulse Test Coefficients

Pulse	A	C	D	E	F
1st Even	-0.693	0.845	-0.675	-3.4	0.135
1st Odd	-0.85	0.56	-0.325	-4.5	0.125
All other even	0.72	0.83	-0.675	-3.5	0.115
All other odd	-0.845	0.56	-0.325	-4.7	0.123

Analysis of pulse test data from the bottom zone (PB1) of Well 10056B is presented here as an example calculation. Data from all other zones in Wells 10056A and 10056B were calculated in a similar manner and the coefficients are presented in Table 4. The definition of parameters used in analyzing the pulse test are shown in Figure 53 for the response of PB1.

After drawing the slopes and measuring time lags and response amplitude for the first even pulse (pulse No. 0), time lag (t_ℓ) was found to be about 4 hours and squared pressure response (Δp^2) was found to be 1.0×10^4 Psi^2. Dimensionless time lag is calculated by

$$t_{\ell D} = \frac{t_\ell}{\Delta t_{cyc}} = \frac{4\ (hrs)}{48\ (hrs)} \simeq 0.0833$$

The next step is to calculate the dimensionless cycle period using the equation relating Δt_{cycD} to $t_{\ell D}$ and suitable coefficient from the above table.

$$\begin{aligned} \Delta t_{cycD} &= C t_{\ell D}^{A} + D \\ &= 0.845\ (0.0833)^{-0.693} - 0.675 \\ &\simeq 0.845\ (5.57) - 0.675 \\ &\simeq 4.05 \end{aligned}$$

From the dimensionless cycle period, Δt_{cycD}, the dimensionless response amplitude can be calculated using the following equation.

$$\begin{aligned} \Delta p_D &= H \left[F \exp\ (E t_{\ell D}) + 0.01 \right] \times \Delta t_{cycD} \\ &= \left[0.135 \exp\ (-3.4 \times 0.0833) + 0.01 \right] \times 4.05 \\ &= 0.4524 \end{aligned}$$

From the definition of dimensionless response amplitude given by

$$\Delta p_D = \frac{k_f h \quad \Delta p^2}{712 \; q\mu ZT}$$

the permeability is calculated as follows:

$$k_f = \frac{712 \; q\mu ZT\Delta p_D}{h\Delta p^2} = \frac{(712)(19)(.0115)(554)(.4524)}{(56)(1.0 \times 10^4)}$$

$$= .0696 \text{ md}$$

The storativity is determined in a similar manner by using dimensionless cycle period

$$\phi c_t = \frac{k\Delta t_{cyc} \text{ (min)}}{56900 \; \mu r^2 \Delta t_{cycD}}$$

$$= \frac{(0.0696)(48)(60)}{(56900)(0.0115)(118)^2(4.05)}$$

$$= 5.43 \times 10^{-6} \text{ (psi}^{-1}\text{)}$$

The same procedures are applied for the first even and odd, the second even and odd, and the third even pulses. The results are presented in Table 5 with dimensionless pressure and cycle values.

Even through the results show some inconsistency in permeability and storativity of individual cycles, permeability as predicted appears to be underestimated and storativity overestimated compared to the results from drawdown interference analysis.

Wellbore storage and skin effects at the pulsing well and under- or overestimation of time lag and response significantly affected the results.

Table 5: Pulse Test Parameters

PA1	1st Even	1st Odd	2nd Even	2nd Odd	3rd Even
t_ℓ (hrs)	1	1.2	0.8	1.3	0.5
$t_{\ell D}$	0.02083	0.035	0.01667	0.0271	0.01042
Δp^2 (psi^2)	0.3525×10^{-5}	0.358×10^{5}	0.388×10^{5}	0.418×10^{5}	0.447×10^{5}
Δt_{cycD}	11.6707	12.5511	14.6606	11.6543	20.7545
Δp_D	1.5853	1.4319	1.8702	1.3923	2.7023
k_f(md)	0.06922	0.06161	0.07418	0.05126	0.09304
$\phi_f c_t$(psi^{-1})	1.67×10^{-6}	1.38×10^{-6}	1.43×10^{-6}	1.24×10^{-6}	1.26×10^{-6}

PA2	1st Even	1st Odd	2nd Even	2nd Odd	3rd Even
t_ℓ (hrs)	4.0	5.5	3	5.3	2.5
$t_{\ell D}$	0.08333	0.1146	0.0625	0.1104	0.05208
Δp^2 (psi^2)	4.44×10^{3}	4.23×10^{3}	4.57×10^{3}	4.94×10^{3}	5.22×10^{3}
Δt_{cycD}	4.0514	3.2150	5.3097	3.3272	6.1392
Δp_D	0.04534	0.2622	0.5837	0.2891	0.6980
k_f(md)	0.003523	0.002139	0.004407	0.002019	0.004613
$\phi_f c_t$(psi^{-1})	2.53×10^{-7}	1.87×10^{-7}	2.34×10^{-7}	1.71×10^{-7}	2.12×10^{-7}

PA3	1st Even	1st Odd	2nd Even	2nd Odd	3rd Even
t_ℓ (hrs)	5.5	8.5	5.5	9.5	4.5
$t_{\ell D}$	0.1146	0.1771	0.1146	0.1979	0.09375
Δp^2 (psi^2)	3.25×10^{3}	2.96×10^{3}	3.10×10^{3}	3.44×10^{3}	3.60×10^{3}
Δt_{cycD}	3.1159	2.1221	3.2122	1.9051	3.8092
Δp_D	0.3169	0.1382	0.2990	0.1201	0.3789
k_f(md)	0.0002680	0.0001283	0.0002652	0.000096	0.0002893
$\phi_f c_t$(psi^{-1})	2.42×10^{-8}	1.70×10^{-8}	2.3×10^{-8}	1.42×10^{-8}	2.14×10^{-8}

Table 5 - Continued

PB1	1st Even	1st Odd	2nd Even	2nd Odd	3rd Even
t_ℓ (hrs)	4	4.5	35.	5	3
$t_{\ell D}$	0.08333	0.09375	0.07292	0.1042	0.0625
Δp^2 (psi^2)	1.095×10^4	1.035×10^4	1.115×10^4	1.24×10^4	1.327×10^4
Δt_{cycD}	4.0514	2.8718	4.6877	3.5116	5.3097
Δp_D	0.4524	0.3410	0.4984	0.3124	0.5837
k_f(md)	0.0696	0.0507	0.0688	0.03877	0.0678
$\phi_f c_t$(psi^{-1})	5.43×10^{-6}	4.14×10^{-6}	4.63×10^{-6}	3.49×10^{-6}	4.04×10^{-6}

PB2	1st Even	1st Odd	2nd Even	2nd Odd	3rd Even
t_ℓ (hrs)	17	18	18	19	18
$t_{\ell D}$	0.3542	0.375	0.375	0.3958	0.375
Δp^2 (psi^2)	0.77×10^3	0.73×10^3	0.85×10^3	0.9×10^3	1.27×10^3
Δt_{cycD}	1.0600	0.9700	0.9964	0.9163	0.9964
Δp_D	0.0539	0.03306	0.04286	0.03018	0.04286
k_f(md)	0.002415	0.001563	0.001730	0.001157	0.001164
$\phi_f c_t$(psi^{-1})	7.1×10^{-7}	5×10^{-7}	5.4×10^{-7}	3.9×10^{-7}	3.6×10^{-7}

2.5 Reservoir Anisotropy

All offset well test data analyses so far have been based on the assumption that the reservoir system is isotropic and homogeneous. However, even if these conditions are not satisfied, the analyses presented in the previous sections will generally provide average-type properties within the reservoir. Based on work originally done by Papadopulos[24], Ramey[25] presented a method for estimating anisotropic properties from interference test data. For complete anisotropic analysis at least three offset wells are required. However the major and minor permeabilities with their angles may be calculated provided porosity-compressibility, ϕc_t, is known or assumed.

The basic equation for the analysis is

$$p\ (t,x,y) = p_i - \frac{141.2\ qB\mu}{\sqrt{k_{max}k_{min}}\,h}\ p_D\left(\left[\frac{t_D}{r_D^{\,2}}\right]_{dir}\right) \tag{7}$$

where the definition of

$$\left(\frac{t_D}{r_D^{\,2}}\right)_{dir} = \frac{2.637 \times 10^{-4}\ t}{\phi\mu c_t}\left[\frac{k_{max}k_{min}}{(k_x y^2 - k_y x^2 - 2k_{xy}\ xy)}\right] \tag{8}$$

In the above equation, k_x, k_y, and k_{xy} are components of the symmetrical permeability tensor aligned with the coordinate system. Ramey suggested the following procedures based on this relationship.

The first step is type curve matching of the observation wells data. Each data set must be matched and pressure match point [Δp, (p_D)] should be the same for all observation well responses. The time match point however, [t, $(t_D/r_D^{\,2})$] will be different for each set of observation well data. The average permeability is estimated from the same pressure match point using the following equation for real gas reservoirs:

$$\bar{k} = \sqrt{k_{max}k_{min}} = \frac{1422\ q\mu ZT\ (p_D)_{m.p.}}{h\ (\Delta p^2)_{m.p.}} \tag{9}$$

The next step is to set equations for each of the time match points using a rearranged version of Equation 10.

$$y^2k_x + x^2k_y - 2xy\,k_{xy} = \frac{2.637 \times 10^{-4}\,k_{max}\,k_{min}}{\phi\mu c}\,\frac{t_{m.p.}}{(t_D/r_D^2)_{m.p.}} \qquad (10)$$

With another relationship,

$$k_xk_y - k_{xy}^{\;2} = k_{max}k_{min} = \bar{k}^2 \qquad (11)$$

If k_x, k_y, and k_{xy} are estimated with $\phi\mu c_t$, the final step will be taken to complete the analysis by estimating the maximum and minimum directional permeabilities and the angle of orientation, using the following equations:

$$k_{max} = 0.5\left\{(k_x+k_y) + \left[(k_x-k_y)^2 + 4k_{xy}^{\;2}\right]^{1/2}\right\} \qquad (12)$$

$$k_{min} = 0.5\left\{(k_x+k_y) - \left[(k_x-k_y)^2 + 4k_{xy}^{\;2}\right]^{1/2}\right\} \qquad (13)$$

$$\text{and}\quad \theta = \arctan\left(\frac{k_{max} - k_x}{k_{xy}}\right) \qquad (14)$$

These procedures are applied to drawdown interference for the bottom zones of Wells 10056A and 10056B. As described in Section 2.3 (Interference Data Analysis) type-curve matching is completed for these two data sets.

According to Ramey, nearly identical pressure match points are obtained from both data sets with different time match points. From the pressure match point, average permeability for the bottom zone is calculated as follows:

$$\bar{k} = \sqrt{k_{max}k_{min}} = \frac{1422\ q\mu ZT\ (p_D)_{m.p.}}{h\ (\Delta p^2)_{m.p.}}$$

$$= \frac{(1422)(19)(0.0115)(0.95)(554)(0.25)}{(56)(10^4)}$$

$$= 0.073 \text{ md}$$

$$k_{max}k_{min} = 0.005329 \text{ md}^2$$

The next step involves setting up two sets of equations from two different time points. As discussed in previous sections, since the range of ω is known, the range of $\phi_f c$ is determined as $2 \times 10^{-7} < \phi_f c < 2 \times 10^{-6}$ (psi^{-1}). These values are substituted into Eq. 10 with well location coordinates shown below.

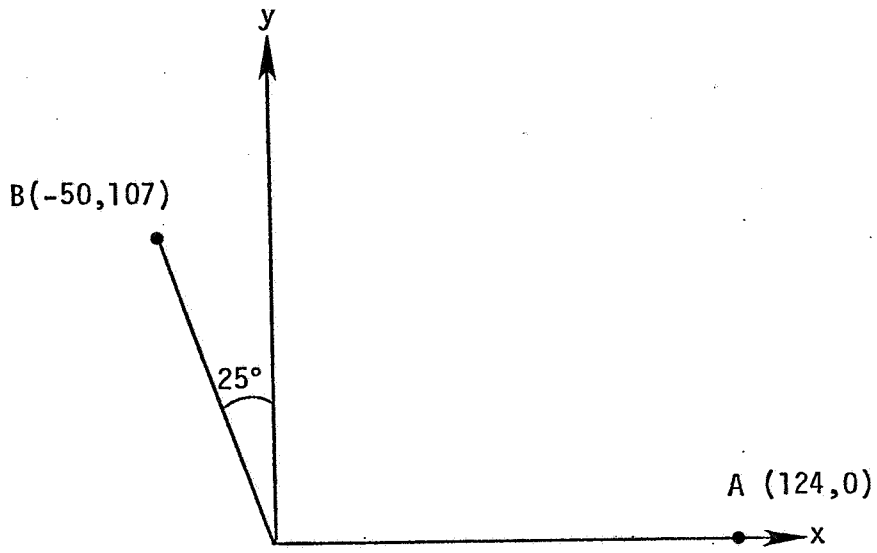

For example, using $\phi_f c$ of 4.4×10^{-7} (psi^{-1}) ($\omega \simeq 2.2 \times 10^{-2}$) and well location A, k_y is calculated by time match point, for Well 10056A [10^3 hrs, 710].

$$(0)^2 k_x + (124)^2 k_y - 2(124)(0) k_{xy} = \frac{(2.637 \times 10^{-4})(0.005329)(10^3)}{(4.4 \times 10^{-7})(0.0115)(710)} \qquad (15)$$

$$k_y = 0.02544$$

Similarly, from the location of Well 10056B and time match point (10^3 hrs, 110) the following equation is set:

$$(107)^2 k_x + (-50)^2 k_y - 2(-50)(107) k_{xy} = \frac{(2.637 \times 10^{-4})(0.005329)(10^3)}{(4.4 \times 10^{-7})(0.0115)(110)} \qquad (16)$$

Substituting k_y into the above equation results in

$$k_x = 0.215 - 0.9346\ k_{xy}$$

This relationship is substituted into Eq. 11 as

$$k_{xy}^2 + 0.02378\ k_{xy} - 0.000141 = 0$$

Solving this quadrature and taking the positive solution gives k_{xy},

$$k_{xy} = 0.00487$$

Then, k_x can be obtained by substituting k_{xy} back into the k_x relationship with k_{xy}.

$$k_x = 0.2104$$

Finally, maximum and minimum permeabilities and orientation are obtained using Eqs. 12, 13, and 14.

$$k_{max} = 0.5\ \{(.2104+.02544)+[(.2104-.02544)^2+4(.00487)^2]^{1/2}\}$$
$$= 0.2105\ (md)$$

$$k_{min} = 0.5\ \{(0.2104+0.02544)-[(0.2104-0.02544)^2+4(.00487)^2]\}$$
$$= 0.02544\ (md)$$

$$\theta = \arctan\left(\frac{0.2105 - 0.02544}{0.00487}\right)$$

$$= 1.5^o$$

These results are shown in the following schematic:

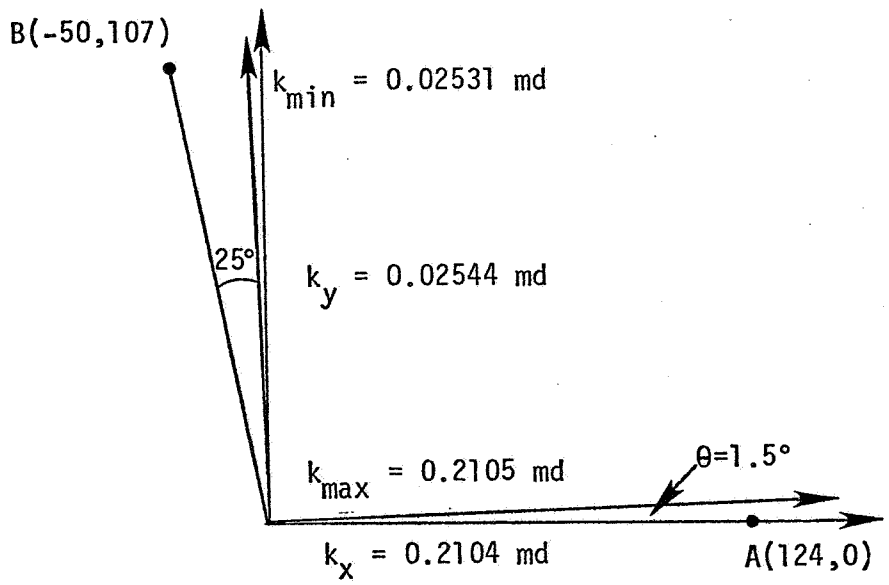

The orientation of the major permeability axis was found to be 1.5^{o} (θ), from the expected maximum permeability axis on which Well 10056A was drilled. The k_{max}/k_{min} ratio was 8.3.

This result was derived using a $\phi_f c_f$ product of 4.4×10^{-7} psi^{-1} (ω = 2.2×10^{-2}). With smaller values of $\phi_f c_f$, the k_{max}/k_{min} ratio increases as does the angle θ. If a value of $\phi_f c_f$ larger than 4.5×10^{-7} is used, the solution of the quadrature for k_{xy} results in a complex number. Results from sensitivity analysis varying $\phi_f c_f$ are shown in Table 6.

Table 6: Sensitivity Analysis Varying $\phi_f c_f$ for Permeability Anisotropy

$\phi_f c_f$ (psi^{-1})	ω	k_{max} (md)	k_{min} (md)	θ
4.4×10^{-7}	2.2×10^{-2}	0.2105	0.02531	1.5^{o}
2.0×10^{-7}	1.0×10^{-2}	0.4020	0.01325	19.4^{o}
1.0×10^{-7}	5.0×10^{-3}	0.7997	0.00664	21.4^{o}
4.5×10^{-7}	2.25×10^{-2}	0.2158	0.02470	-1.7^{o}
4.5×10^{-7}	2.25×10^{-2}	Complex Values Obtained		

From this sensitivity study, the range of $\phi_f c_f$ (ω) $4.4 \times 10^{-7} < \phi_f c_f < 4.5 \times 10^{-7}$ (which is equivalent to $2.2 \times 10^{-2} < \omega < 2.25 \times 10^{-2}$) is very reasonable considering the geologic and fracture lineament studies done in the area.

2.6 Reservoir Drainage Volume

Average pressure, $\bar{p}$, is fundamental in characterizing reservoir volume, estimating drainage volume, and predicting future reservoir behavior. Average pressure could not be determined in this case, since most of the buildup, drawdown, and interference tests show no apparent boundary effects.

An attempt is made to establish average pressure, based on the assumption that at the end of the buildup test, control well pressure had reached pseudo-steady state.[27] For a closed system, in which the well is located at the center of a circular reservoir, Cobb and Smith[28] shows that the average reservoir pressure will be reached after sufficient shut-in time. This relationship is expressed as,

$$\Delta t_{DA} = (t_{DA})_{pss}$$

where $(t_{DA})_{pss}$ is given as 0.1. This relationship was modified and verified by Dr. Raghavan [27] to be applied to the naturally fractured reservoir as follows:

$$\frac{\Delta t_{DA}}{\omega} = (t_{DA})_{pss}$$

As shown in Section 2.2 (Control Well Analysis), average permeability was 0.02 md based on a formation thickness of 155 ft. Substituting for dimensionless shut-in time results in

$$\frac{0.000264\ kt}{(\phi_f c_f + \phi_m c_m)\omega\mu A} = (t_{DA})_{pss} = 0.1$$

The terms in the denominator, $(\phi_f c_f + \phi_m c_m)\ \omega$, are equivalent to $\phi_f c_f$ using the definition of ω. The fracture porosity is unknown and matrix porosity is much greater than fracture porosity. The total porosity is assumed to be 1.0%, based on core analysis performed by Core Labs. Since ω is known to be in the range of 0.01 to 0.1, it is assumed to be 0.05% for this calculation. By substitution the drainage radius is calculated as follows:

$$(t_{DA})_{pss} = \frac{(0.000264)(0.02)(1172)}{(0.01)(.05)(0.002)(0.0115)\pi r_e^2} = 0.1$$

Reservoir stabilization time was determined to be 1172 hours. Stabilization was established at the point when pressure was increasing an average 0.48 psi/day. From the above calculation, the drainage is

$$r_e = \sqrt{\frac{(.000264)(.02)(1172)}{(0.01)(.05)(0.002)(0.0115)(\pi)(0.1)}} \simeq 1300 \text{ ft}$$

Thus, the drainage volume is approximately

$$V_p = 8.2 \times 10^6 \text{ cu.ft.}$$

This value should be taken as an average point for drainage volume. For the possible range of ω the drainage radius and volume may be calculated as follows:

$$925 < r_e < 2926 \text{ ft}$$
$$4.2 \times 10^6 < V_p < 4.2 \times 10^7 \text{ cu.ft.}$$

A second procedure referred to as the method of images (or reflection of well on a boundary) is applied. The reservoir limit may be determined from the interference test data assuming that all test data from the bottom zone of Well 10056A are matched to the line source solution. The procedure to determine the nearest distance to the boundary is presented by Ramey, et al.[29] The relationship for determining limit is given by:

$$p_D = \frac{k_h}{1422\ q\mu TZ} (p_{ws}^2 - p_{wf}^2)$$

$$= \frac{(.0693)(56)}{(1422)(18.43)(.0115)} \frac{(1.17 \times 10^5)}{(554)\ (.95)}$$

$$= 2.87$$

The next step is to determine the argument for an Exponential Integral with one percent of the computed pressure drop.

$$0.01\ (p_D) = 0.01\ (2.87) = 0.0287$$

The distance is computed from

$$-Ei(-a_{2D}2/\ \Delta t_D) = 2(0.0287) - 0.574$$

From the exponential table,

$$a_{2D}^2/4t_D \simeq 1.88$$

$$a_2^2 = \frac{4(2.637 \times 10^{-4})kt}{\phi\mu c_t} \times (1.88)$$

$$= \frac{4(2.637 \times 10^{-4})(.0693)(907)}{(.0009)(.0115)(\frac{1}{500})}\ (1.88)$$

$$= 6.02 \times 10^6$$

$$a_2 \simeq 2454 \text{ feet}$$

It should be noted that this solution is based on the assumption that even though all of the test data are matched to the line source solution, the last portion of data is affected by this boundary.

Compared to the first method, which is based on the assumption that the control well buildup pressure reaches the pseudo-steady state, the second method is less reliable.

Thus, the drainage volume of 8.2×10^6 cu ft calculated by the first method is used in this analysis for simulation and study of the drainage pattern.

3.0

WELL TEST ANALYSIS - NUMERICAL STUDY
ESTIMATION OF RESERVOIR PARAMETERS BY HISTORY MATCHING

3.0 WELL TEST ANALYSIS - NUMERICAL STUDY
ESTIMATION OF RESERVOIR PARAMETERS BY HISTORY MATCHING

During the course of the project, radial flow simulations were used to determine offset well locations and to design drawdown and buildup interference tests. The first simulations utilized data from the August 1980 30-day buildup test at the control well. The known pressure history of the control well from the end of the buildup test until shut-in in March 1981 provided the necessary boundary conditions for the simulation runs in this study. Both radial and two-dimensional simulation models were employed to obtain estimates of shale parameters by history matching interference data at the two offset wells (10056A and 10056B) approximately 120 feet from the control well (10056). A major consideration was to characterize the known reservoir anisotropy as determined by pressure response at the two offset wells which formed an angle of approximately 120 degrees with the control well.

Both the radial model "SUGAR" and the two-dimensional model "SUGAR-MD" were used to history-match drawdown and buildup interference data. These models were presented in detail in earlier reports.[30,31] They are identical except for geometrical and plotting options. SUGAR-MD is a completely general 2-D cartesian or polar coordinates fractured gas reservoir simulator but has no built-in plotting capability. SUGAR is strictly a radial gas simulator for fractured reservoirs, but has extensive plotting capability included as an integral part of the simulator.

In this study, the radial model (SUGAR) was used where only radial flow could be used, due to its extensive plotting capability. SUGAR-MD had to be used for the two-dimensional simulation required in the determination of reservoir anisotropy. The Warren and Root option, which assumes pseudo-steady-state flow in the shale matrix, was used in both models.

3.1 Radial Flow Simulation

The first phase of the simulation study was to match drawdown and buildup interference data at both offset wells. Because the upper two zones were known to contribute little to production, the bottom zone in each well was

studied. In the interest of computation time and overall efficiency, the radial flow model was used first in order to estimate parameters which would match the response to both offset wells. Also, as the analytical work had indicated psuedo-steady-state flow in the shale matrix, this assumption was incorporated into the numerical model study.

The response in the bottom zone (PB1) of 10056B was first matched utilizing the following properties:

Fracture porosity = .00125, fraction
Fracture permeability = .03 md
Matrix porosity = .01, fraction
Matrix permeability = .1E-06 md
Fracture spacing = 6.6 ft.
Adsorbed gas content - .00700 scf/cu.ft./psia
Klinkenberg parameter = 893 psia
Drainage radius = 800 feet
Skin factor = -2.0

Since radial flow was considered, the fracture system permeability of .03 md must be considered as an average value. A good match was obtained (Figure 56) which illustrates that interference data can be successfully matched with reasonable parameters.

It should be noted that the PB1 response data (bottom zone in Well 10056B) was originally matched without adsorbed gas but with a very high matrix porosity of 10 percent. This occurred because the numerical models (SUGAR and SUGAR-MD) had no provision for adsorbed gas using the simpler pseudo-steady-state (Warren and Root) option. Analytical considerations indicated that an equivalent amount of adsorbed gas could be modeled as free gas to a close approximation for a linear adsorption isotherm curve. Based on work by Battelle Laboratories[32] the quantity of adsorbed gas (up to about 600 psi) from Well 10056A core samples was approximately linear. Thus, an option was added to both models to provide the capability for desorption with pseudo-steady state flow.

Using data from Battelle's core analysis work, a value of .007788 scf/cu ft/psi was obtained, which is equivalent to a free matrix porosity of about 11.7 percent. This value was used together with a measured value of 1 percent

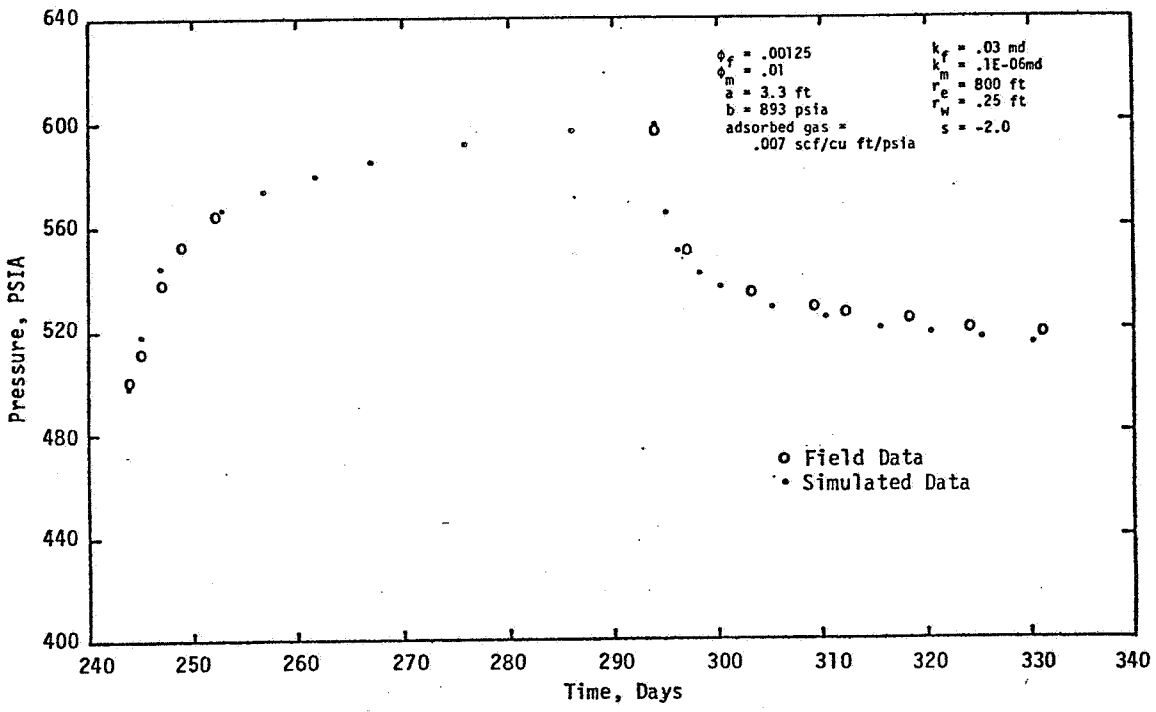

Figure 56: Radial Flow Simulation - History Match of Interference Data in Bottom Zone of Well 10056B

matrix porosity from core analysis by Core Labs (see Appendix) in an attempt to re-match the PB1 response data. It was found that a favorable match could be obtained by reducing adsorbed gas slightly, to .007 cu ft/psi. Except for sensitivity studies, these values for ϕ_m and adsorption were used throughout the remainder of the study. The Klinkenberg factor of 893 psi obtained from Battelle Laboratories' work (which will be discussed later) was constant throughout the study. The skin factor of -2.0 was obtained from buildup analysis at the control well, and drainage radius of 800 feet was estimated from initial history matching of production data at the control well.

After successfully matching the response of PB1, an attempt was made to match the response in the bottom zone of Well 10056A (PA1) by varying only fracture porosity. However, this proved to be impossible due to the large pressure drawdown in Well 10056A at the beginning of the buildup test. The pressure in Well 10056A was only 442 psia, compared to 499 psia in Well 10056B. In order to match the large drawdown in PA1 and the rapid buildup subsequent to shutting in the control well), a larger fracture permeability (.08 md) and a smaller fracture porosity (.0006) had to be used. Figure 57 shows that an approximate match was obtained with all other parameters identical to the PB1 match.

The next step was to determine if the parameters from the match of the PB1 or the PA1 interference data would match the 18-year production history at the control well. With control well pressure as the boundary condition, interference data was independent of net thickness; however, production rate was directly proportional to thickness. From gamma ray logs, a net thickness of 56 feet was determined from the gross zone thickness of 81 feet. However, a slightly different cutoff value would yield a different value of net thickness. Thus a reasonable range would be a net productive shale thickness of about 50 to 60 feet. Since both the PB1 and the PA1 matches were obtained without regard to thickness, there was a question as to whether the proper production rates (25 to 19 MCFD) could be obtained with h in the range of 50 to 60 feet. It was found that with h adjusted to 50 feet using the PB1 matching parameters, the 18-year production history could be matched as shown in Figures 58 and 59.

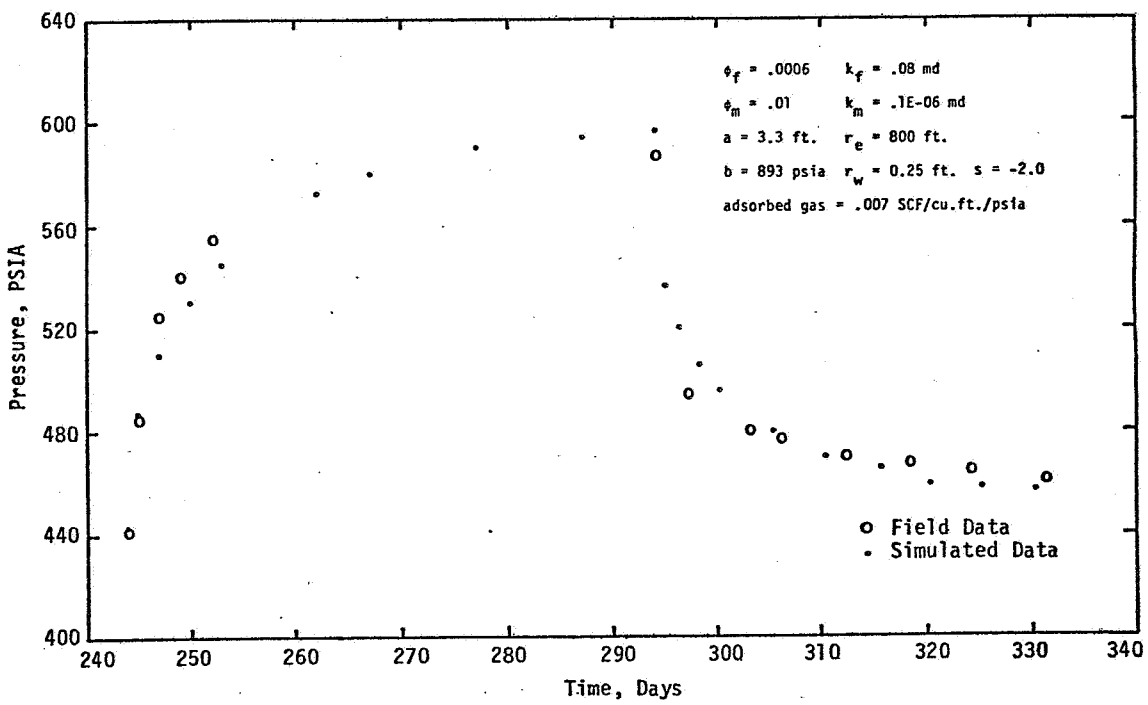

Figure 57: Radial Flow Simulation - History Match of Interference Data in Bottom Zone of Well 10056A

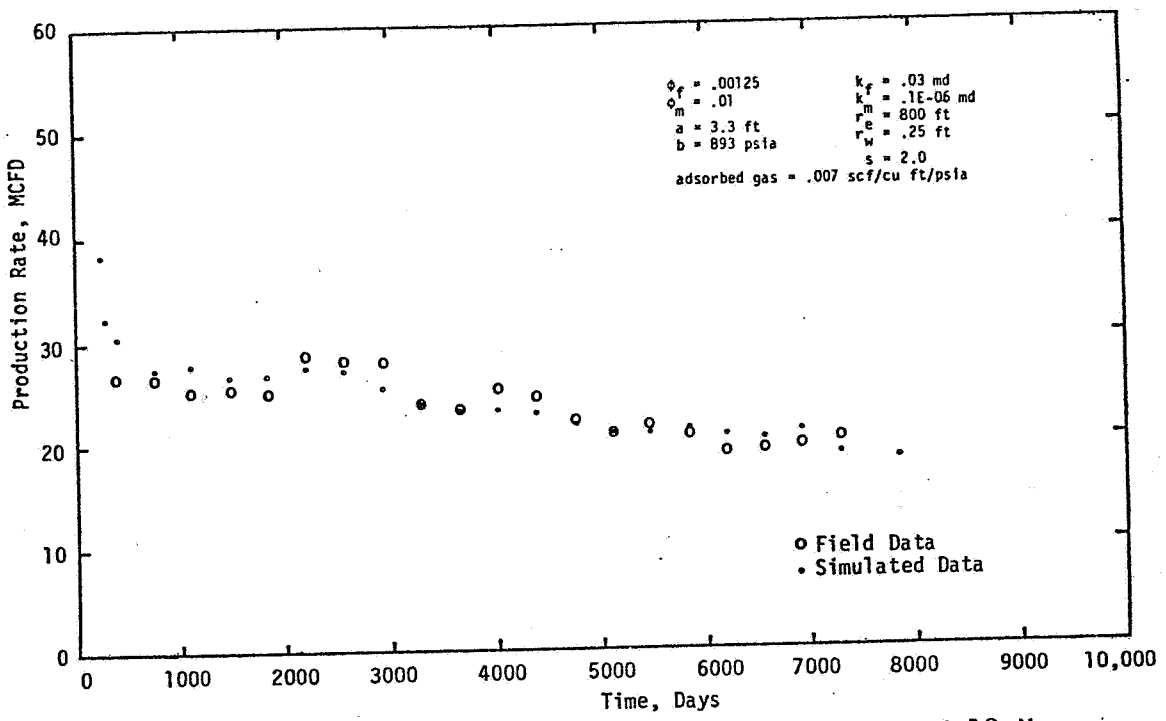

Figure 58: Radial Flow Simulation - History Match of 18-Year Production Decline at Control Well 10056

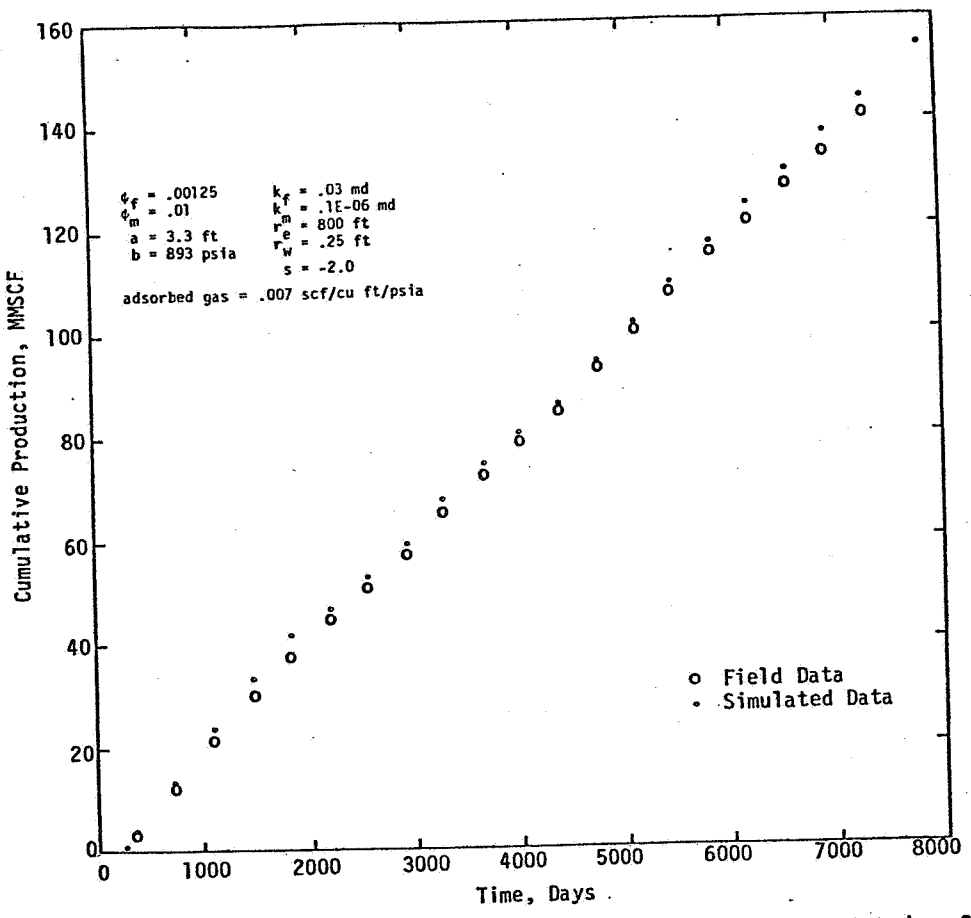

Figure 59: Radial Flow Simulation - History Match of 18-year Cumulative Production at Control Well 10056

3.2 Two-Dimensional Flow Simulation

Having matched both the 18-year production history and the interference response in the bottom zone of Well 10056B with a set of reasonable fracture and matrix parameters (based on laboratory and analytical work) the next step was to use the two-dimensional model (SUGAR-MD) in an attempt to find directional fracture system permeabilities, k_{fx} and k_{fy}, which would give a simultaneous match of the interference data at both offset wells. It was logical to begin with a ratio ($R = k_{fx}/k_{fy}$) of 7 to 10 as indicated from the analytical work and with a mean permeability ($k = k_{fx}\ k_{fy}$) of .03 from the radial flow match of the PB1 data.

The initial grid was very coarse (13 x 11) having grid blocks as large as 40 x 50-feet in the vicinity of the three wells. Subsequently, a 19 x 18 grid-block network was used with 10-foot-square blocks to some distance beyond the offset wells. Table 7 gives details of this grid system. A difference of only 5 psi was obtained at two points in time with the finer grid which was used to generate all subsequent results. The x-direction was arbitrarily chosen in the direction of Well 10056A.

Due to symmetry, only one quadrant needed to be simulated. Although Wells 10056A and 10056B are approximately 120 degrees apart (with reference to the control well) the image location of Well 10056B in the first quadrant would have the same pressure response. Figure 60 shows the quadrant simulated and the grid structure to a point beyond the offset wells.

It was found that a match could be obtained with a large (but finite-acting) drainage area four times the size of that used in the radial flow simulations. A drainage radius of 800 feet was used in the radial flow work; an equivalent square is 1,418 feet on a side of which one quadrant is represented by the grid in Table 7. By increasing the fracture spacing parameter from 3.3 feet, as used in the radial simulations to 7 feet, a fairly good match could be obtained in a 2,836 foot square with reasonable values of h, k_{fx}, and k_{fy}. Figures 61 and 62 show results for this case.

Subsequently, the quadrant was reduced to represent a 1,418-foot square area and the data were rematched. It was only necessary to vary fracture spacing and fracture permeability to obtain the re-match which is shown in Figures 63 and 64. The match at PA1 is considered excellent and both PA1 and PB1 results have been shown to be independent of grid-block size. It is

Table 7: Grid System Used for Final Two-Dimensional Simulations

X-Direction			Y-Direction		
Block Index	Block Size (ft)	Cumulative Distance (ft)	Block Index	Block Size (ft)	Cumulative Distance (ft)
1	1.639	1.639	1	1.639	1.639
2	5.361	7.000	2	5.361	7.000
3	7.	14.	3	5.	12.
4	5.	19.	4	10.	22.
5	10.	29.	5	10.	32.
6	10.	39.	6	10.	42.
7	6.	45.	7	10.	52.
8	10.	55.	8	10.	62.
9	14.	69.	9	10.	72.
10	10.	79.	10	10.	82.
11	10.	89.	11	10.	92.
12	10.	99.	12	10.	102.
13	10.	109.	13	10.	112.
14	10.	119.	14	10.	122.
15	10.	129.	15	30.	152.
16	30.	159.	16	100.	252.
17	100.	259.	17	200.	452.
18	200.	459.	18	247.	709.
19	250.	709.			

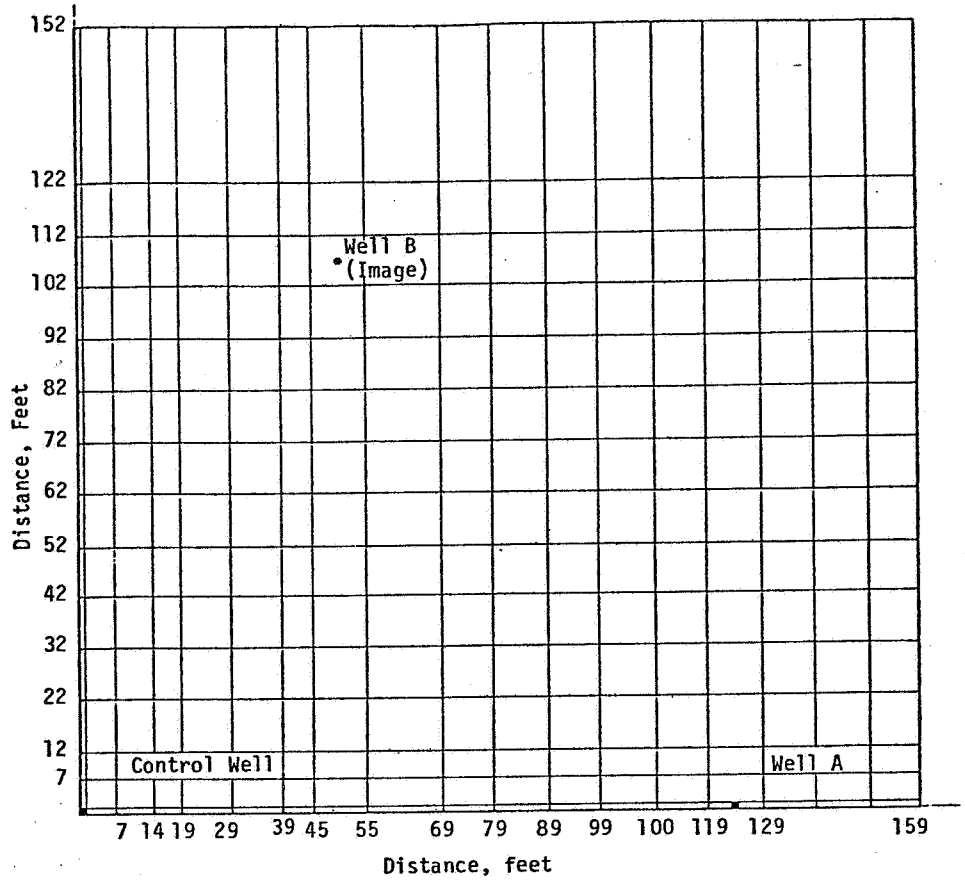

Figure 60: Portion of Finite-Difference Grid Used for Two-Dimensional Simulation

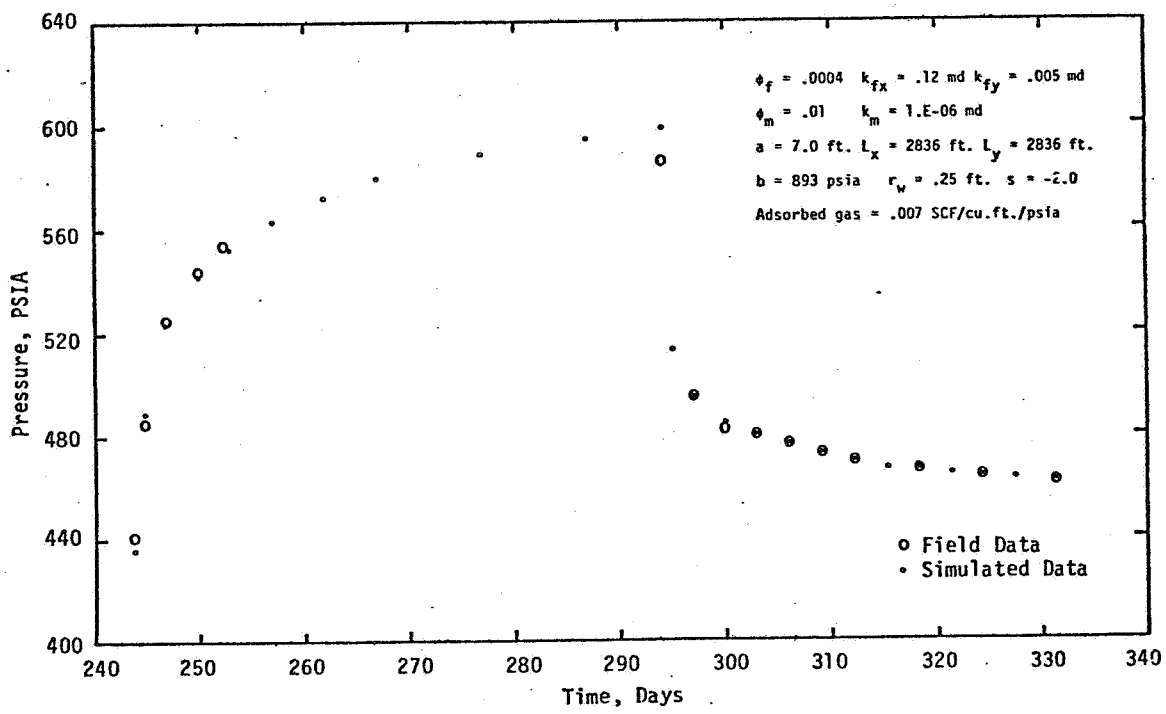

Figure 61: Two-Dimensional Simulation - History Match of Interference Data in Bottom Zone of Well 10056A

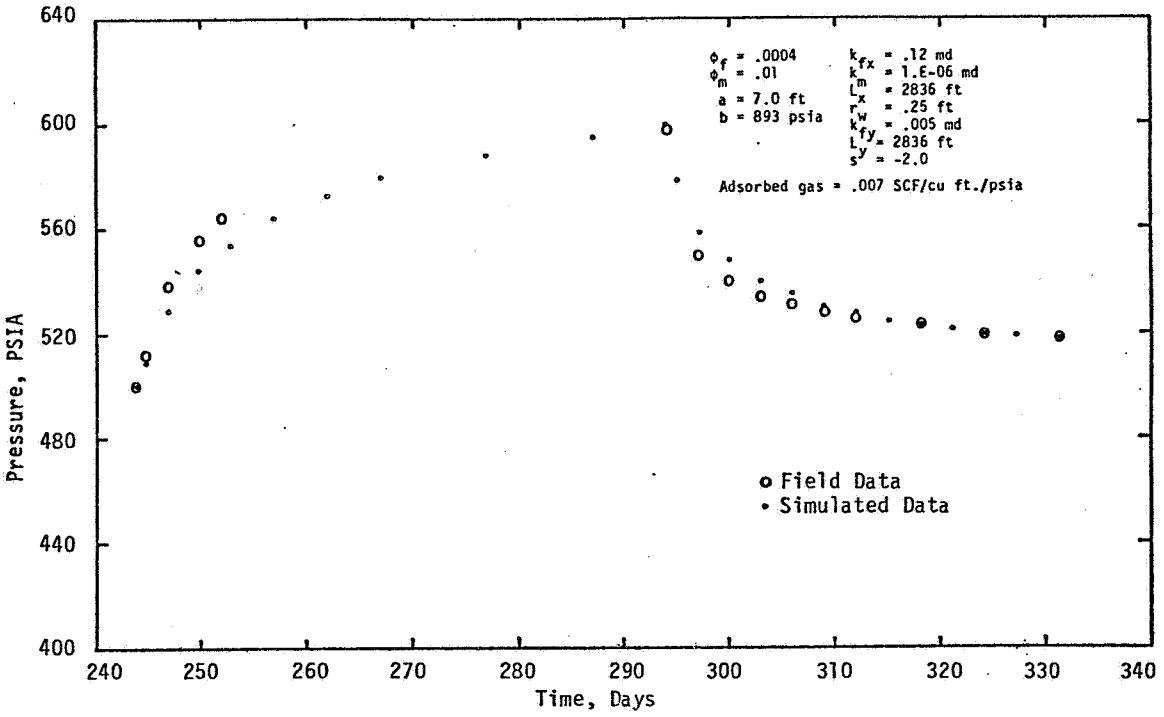

Figure 62: Two-Dimensional Simulation - History Match of Interference Data in Bottom Zone of Well 10056B

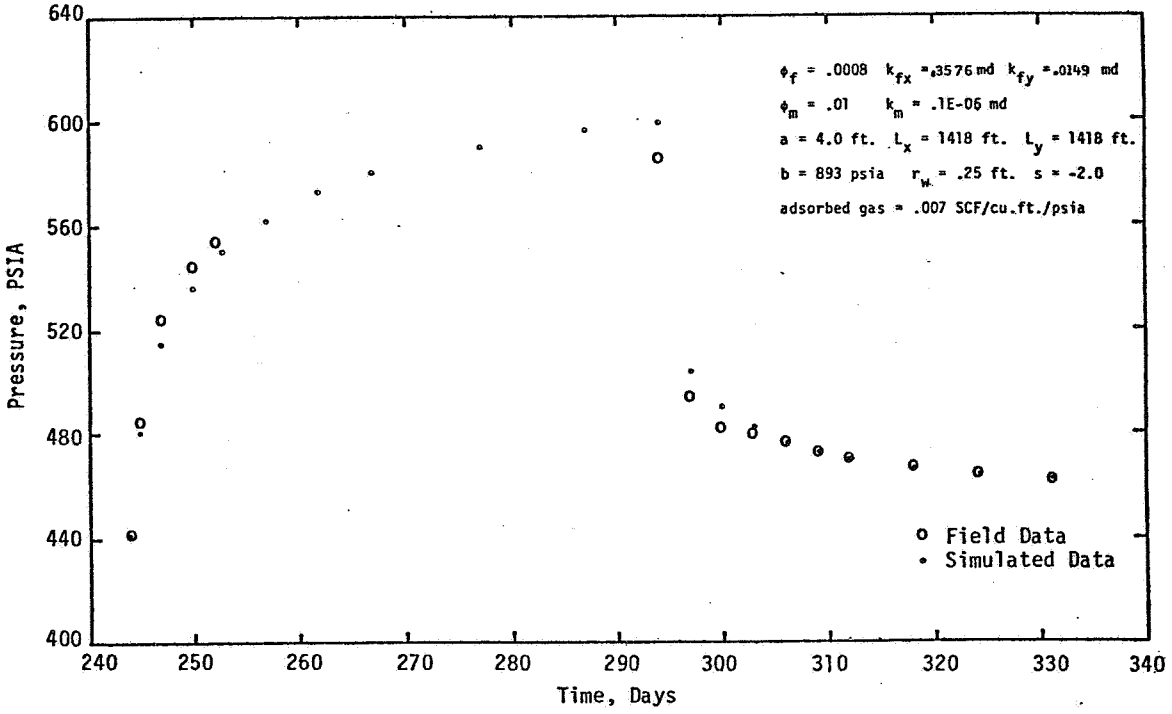

Figure 63: Two-Dimensional Simulation - History Match of Interference Data in Bottom Zone of Well 10056A

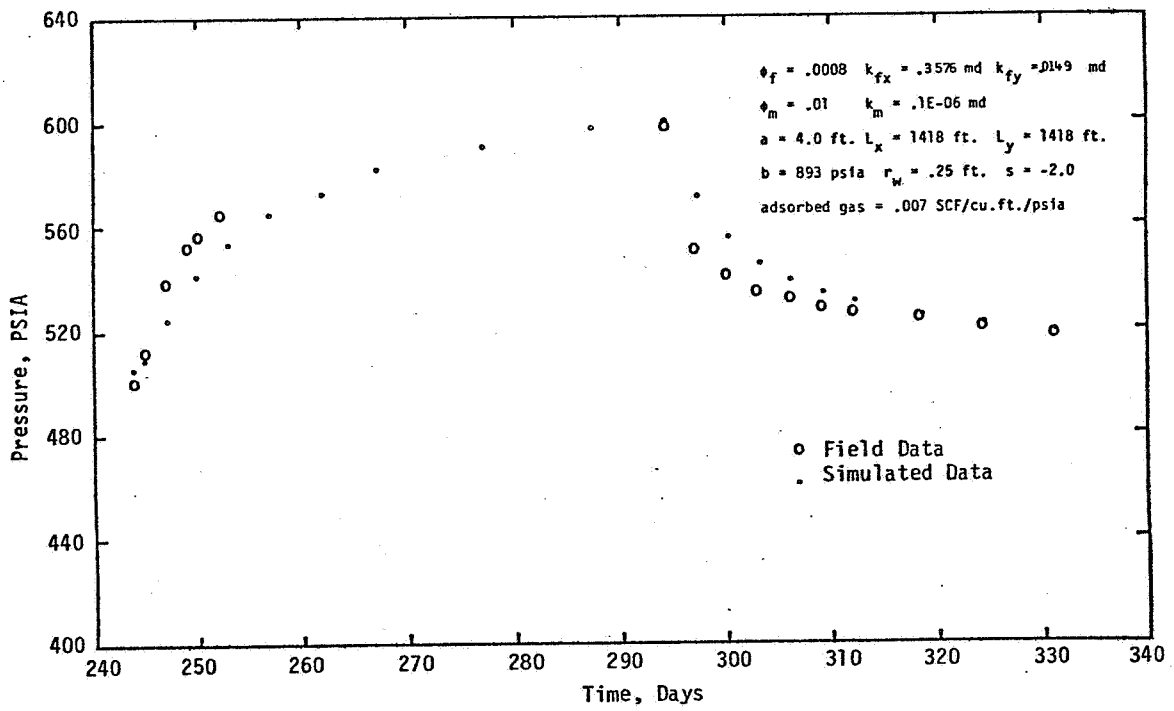

Figure 64: Two-Dimensional Simulation - History Match of Interference Data in Bottom Zone of Well 10056B

likely that with extensive runs and careful study, a better match of the buildup data at PB1 could be obtained.

A sensitivity study was then conducted on the 2D match shown in Figures 63 and 64, varying those parameters which could not be measured accurately in the laboratory or vary widely over the net formation interval.

In Figures 65 and 66, the sensitivity to fracture porosity is illustrated. The characteristics to note are: (1) pressure drawdown is only slightly sensitive to fracture porosity; and (2) a much steeper buildup and a more rapid drawdown result from a decrease in fracture porosity.

The effects of mean permeability and anisotropy are shown in Figures 67 and 68. Changing the anisotropy ratio, R, from 24 to 10 only slightly affects the response in Well 10056A but significantly reduces the pressure drawdown at Well 10056B. However, increasing the mean permeability from .0245 to .0700 significantly increases the pressure drawdown at both offset wells and also alters the shape of the buildup curve.

Figures 69 and 70 show the effect of fracture spacing. The parameter "a" is the radius of the cylindrical element; thus, 2a is the approximate fracture spacing. The entire curve is shifted downward when spacing is doubled. According to the definition of the dimensionless matrix-fracture transfer coefficient λ, this would be equivalent to reducing matrix permeability or increasing fracture permeability by a factor of 4. When fracture spacing is halved, less pressure drawdown and a more rapid buildup occur.

Without adsorbed gas and matrix porosity still at one percent, greater pressure drawdown and more rapid depletion would be expected to occur. This is illustrated in Figures 71 and 72. It should be noted that without adsorbed gas and a matrix porosity of one percent, a 1,418-foot-square does not contain as much gas as the control well (Well 10056) has produced.

Following the sensitivity runs, it was found that due to the method of data entry, the Klinkenberg parameter of 893 psi had been applied to the fracture system as well as the matrix. This is approximately equivalent to an increase in permeability of a factor of 1 + b/p. Taking

$$p = 0.5\ (p_i + p_{wf}) = .5\ (615 - 275) = 445$$

gives 1 + b/p = 3.01. Hence, the effective fracture system permeabilities for the match given in Figures 63 and 64 are approximately k_{fx} = .36, k_{fy} = .015. This gives a mean permeability, k, of .073 md with the ratio unchanged.

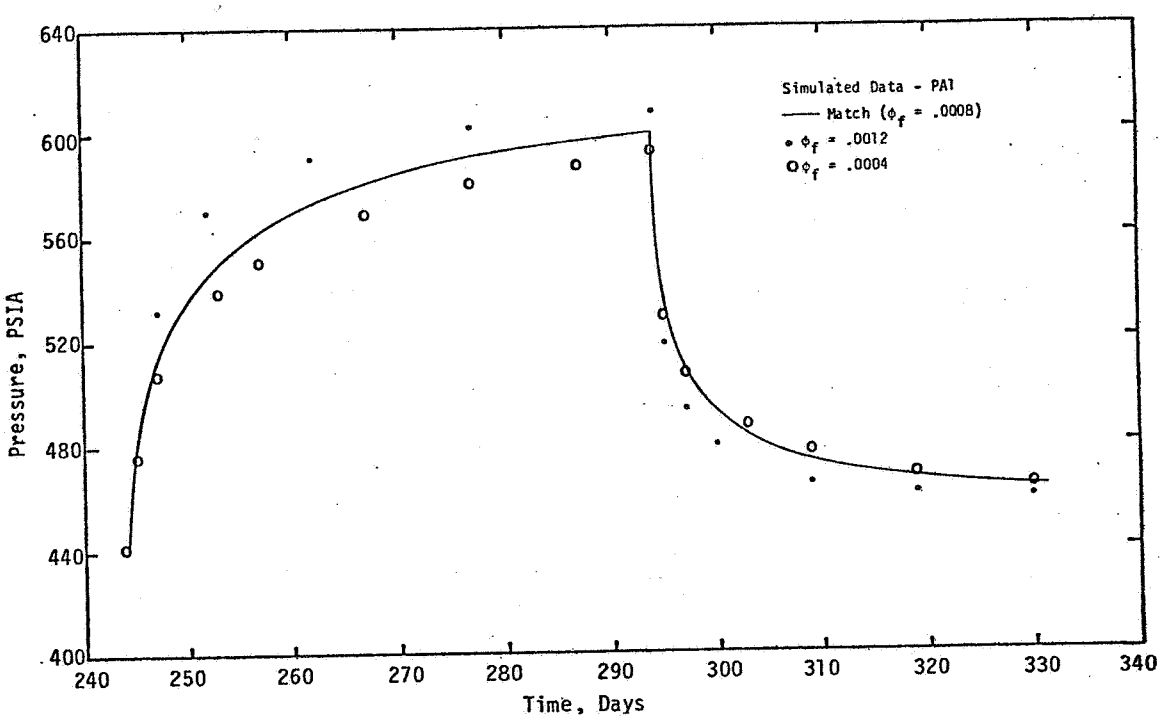

Figure 65: Effect of Fracture Porosity on Interference Data in Bottom Zone of Well 10056A

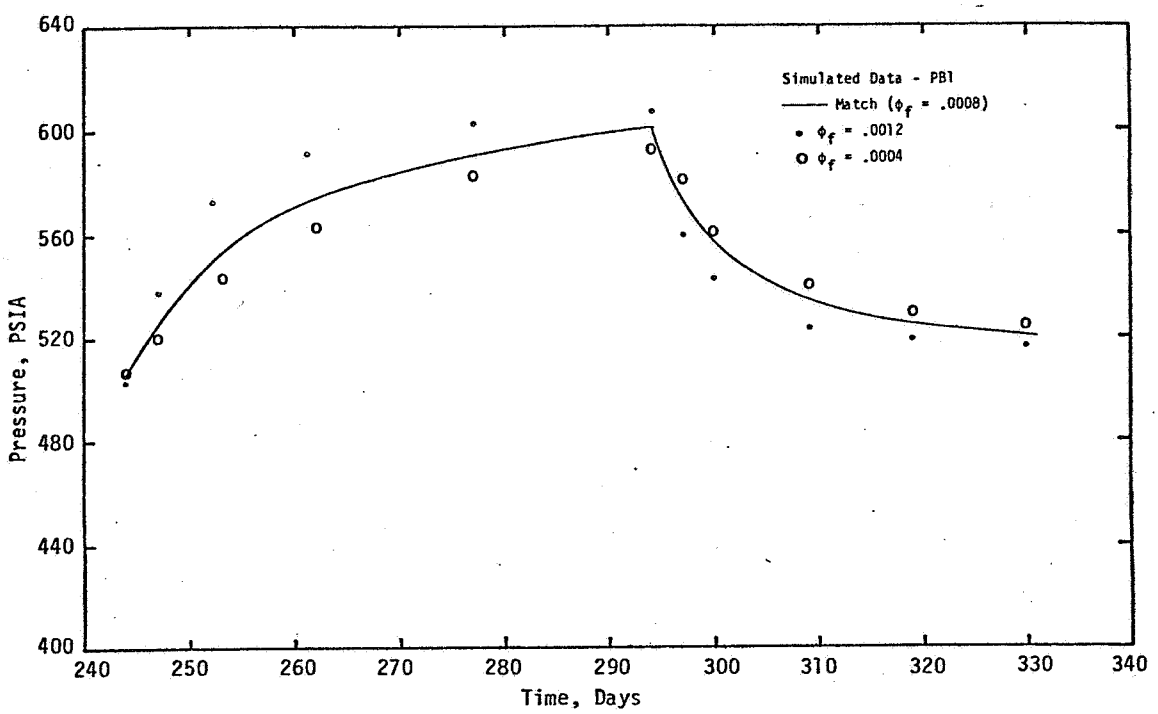

Figure 66: Effect of Fracture Porosity on Interference Data in Bottom Zone of Well 10056B

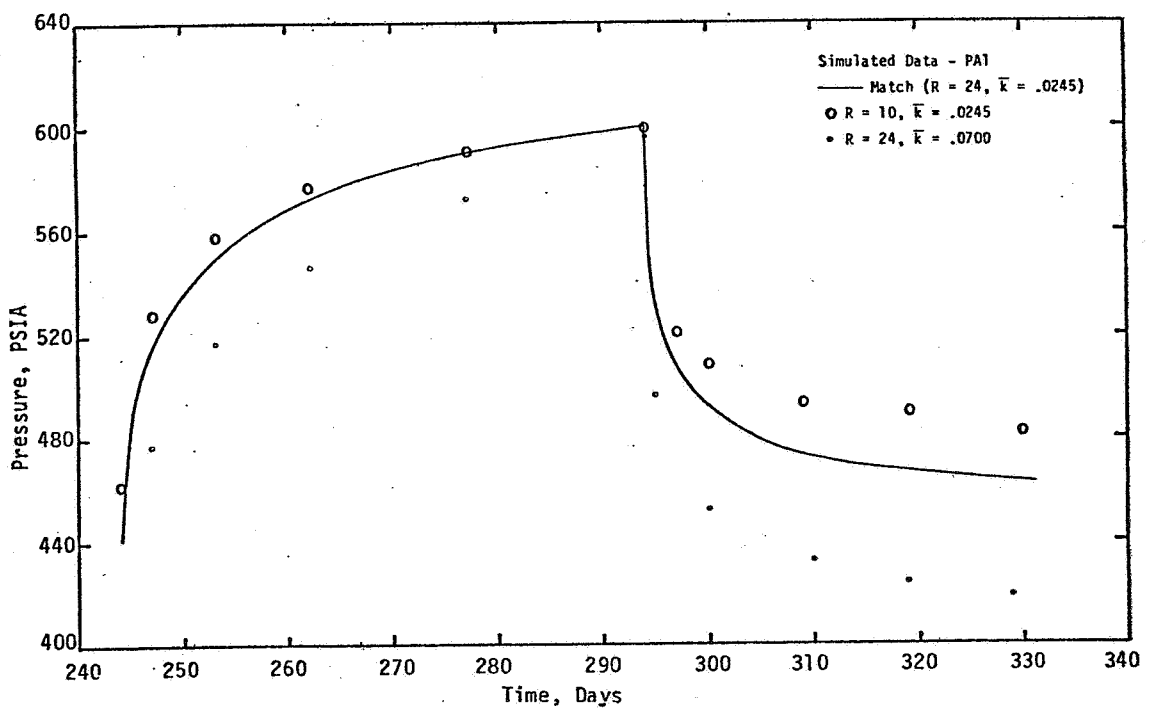

Figure 67: Effect of Anisotropy on Interference Data in Bottom Zone of Offset Well 10056A

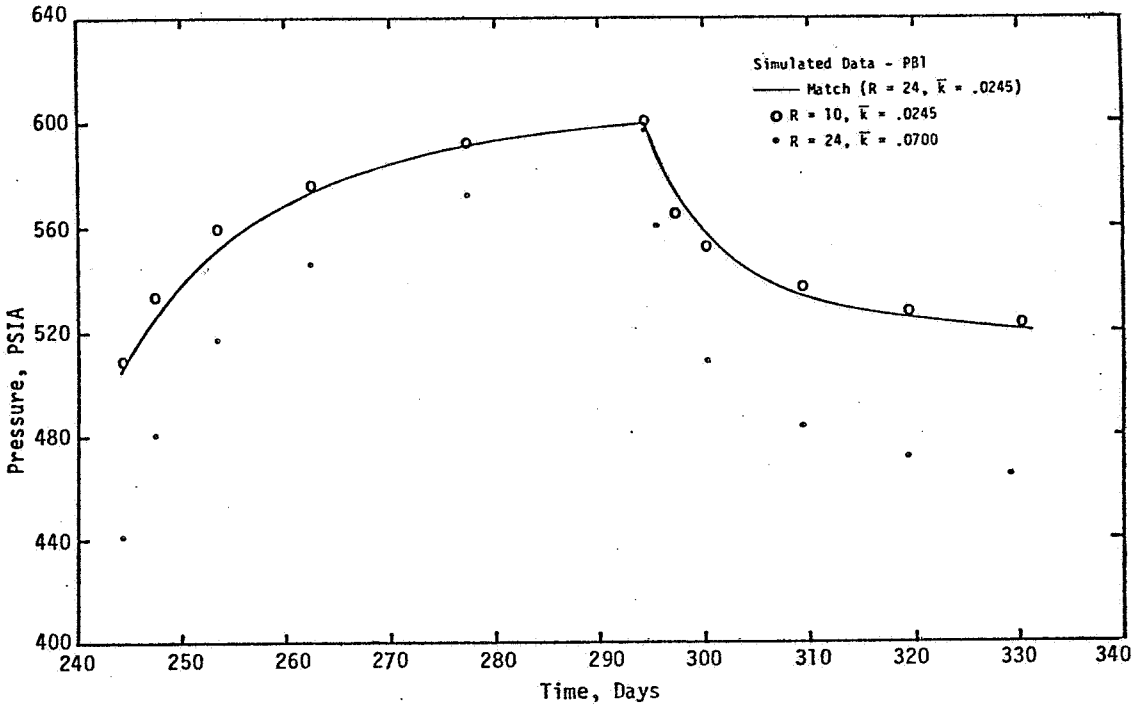

Figure 68: Effect of Anisotropy on Interference Data in Bottom Zone of Well 10056B

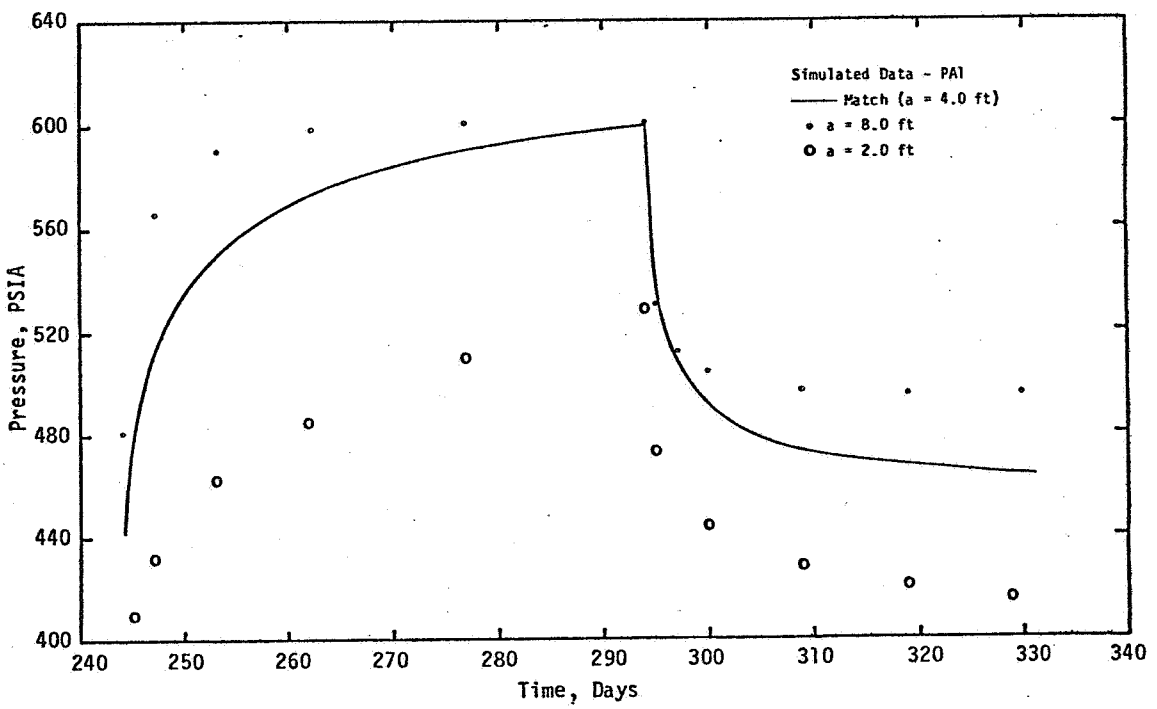

Figure 69: Effect of Fracture Spacing on Interference Data in Bottom Zone of Well 10056A

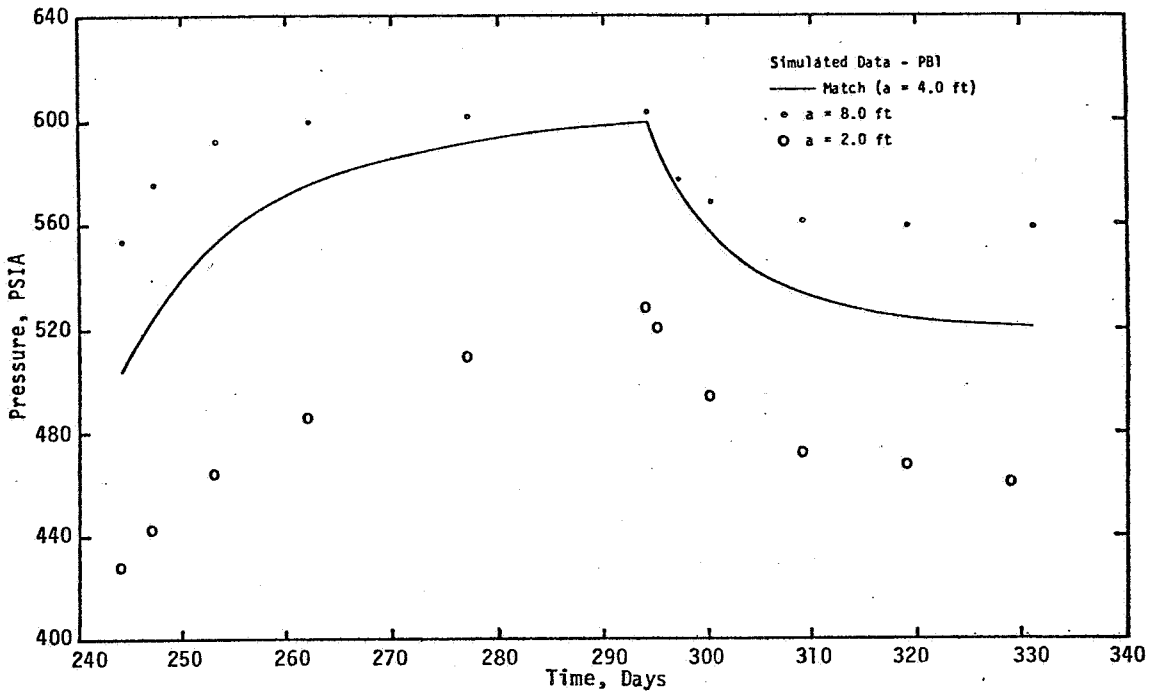

Figure 70: Effect of Fracture Spacing on Interference Data in Bottom Zone of Well 10056B

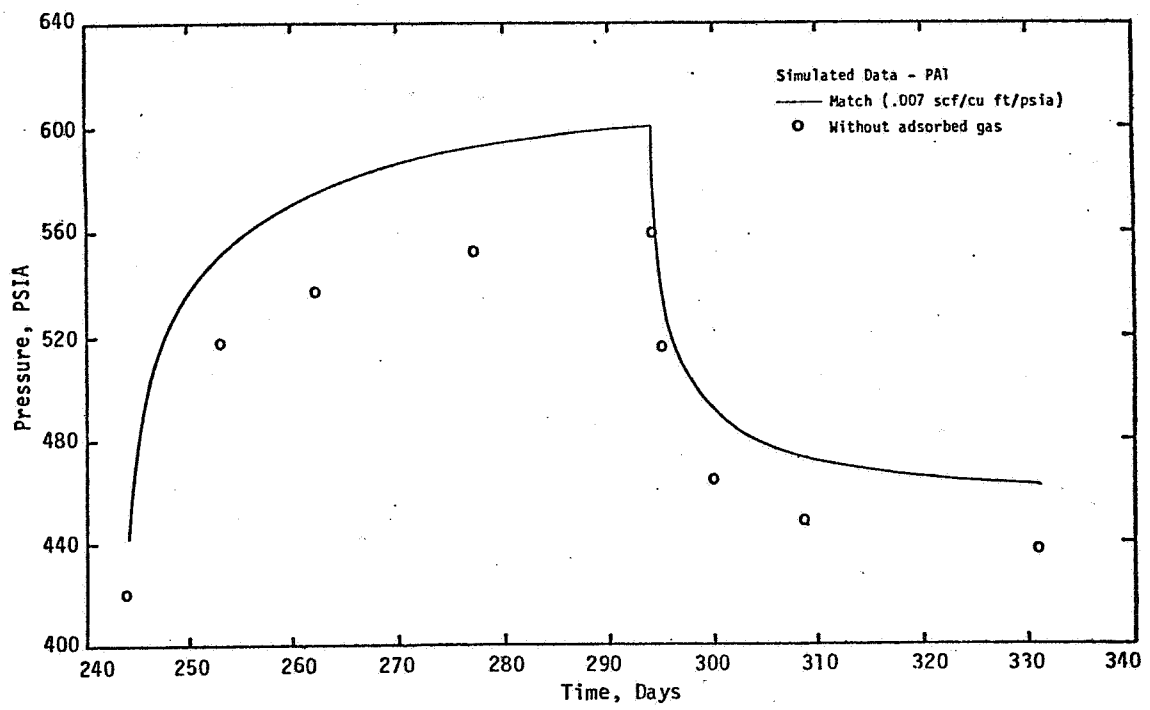

Figure 71: Effect of Adsorbed Gas on Interference Data in Bottom Zone of Well 10056A

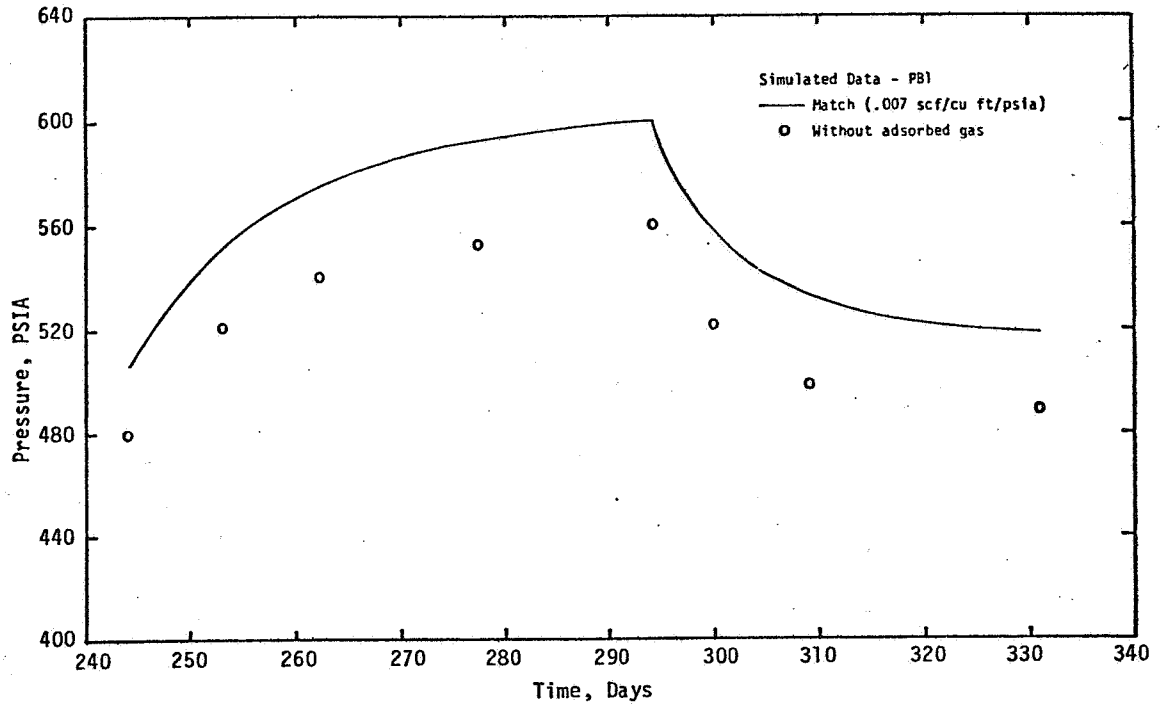

Figure 72: Effect of Adsorbed Gas on Interference Data in Bottom Zone of Well 10056B

A confirmation run was made with the above values of k_{fx} and k_{fy} with b = 893 applied only to the shale matrix. This was accomplished by using the functional form $b = c_1 k_L^{-}$ given by Jones and Owens[33] with k_L = .1E - 06. With c_1 = 12.64 from Jones and b = 893 psi from Coutant,[32] a value of .264 was obtained for c_2. This is close to the value of .33 from Jones' work on western tight sands. Values obtained from the confirmation run gave nearly identical results at PB1 and an approximate match on PA1. Thus, it was not necessary to repeat the sensitivity runs.

4.0

CONCLUSIONS

4.0 CONCLUSIONS

Gas flow in a Devonian shale reservoir should be characterized by a naturally fractured reservoir that has a dual porosity system. In particular, portions of the Meigs County reservoir surrounding Well 10056 are highly fractured, and can be modeled using pseudo-steady-state gas transfer from the matrix system to the fracture system. This finding is consistent with the theory of well testing for the naturally fractured reservoir, since the amount of fracturing in this reservoir is large enough that no noticeable difference can be found in pseudo-steady-state and unsteady state flow under the limit of test time.

- A great deal of confidence can be placed in the values obtained in the flow rate calculation. The following table compares analytical results with field measurement.

Table 8: Analytical and Field Measurements

Zone	(MCFD) Field Measurement	(MCFD) Analytical Method	(MCFD) After Blowout Well A
PA1	12.05	10.97	10.93
PA2	0.672	0.226	0.96
PA3	2.19	0.121	0.46
PB1	4.01	4.06	-
PB2	0.42	0.617	-
PB3	0.05	0.035	-
Control	19.0	19.0	-

The analytical method is given more credibility than the field measurements for the smaller flow rates due to possible error in water level readings and orifice plate changes.

- For the single well analysis at the control well, the analytical results were in very good agreement. Based on a total thickness of 155 feet*, the semilog analysis resulted in a fracture permeability of .0187 md, while the type curve analysis yielded .0200 md. Also, from the type curve analysis, the fracture porosity was calculated to be approximately .09%. These values are shown below. The skin factor from semilog analysis was -2.6 and from type curve analysis -2.0.

	k_f semilog Analysis	k_f type curve Analysis	ϕ_f type curve Analysis	Skin Factor	
				Semilog	Type Curve
Control Well (10056)	.0187 md	.0200 md	.09%	-2.6	-2.0

This range of skin factor does not present a problem since the difference in the shape of each type curve (i.e. skin = -2.0 and skin = -2.6) is minimal; therefore a skin factor of -2.0 was used in the remainder of the work.

- The fracture permeability and fracture porosity for each zone of the offset wells were calculated using buildup and drawdown interference type curve matching. The fracture permeability was also calculated by semilog analysis. The results are shown below based on a net thickness of 56, 63, 36 feet for Zones 1, 2, and 3, respectively.

Table 9: Fracture Permeability and Porosity

Zone	k_f Buildup Type Curve	k_f Buildup Semilog	k_f Drawdown Type Curve	k_f Drawdown Semilog	ϕ_f Buildup Type Curve	ϕ_f Drawdown Type Curve
PA1	.03850	.04938	.07080	.06930	.00050	.00007
PA2	.00135	.00153	.00350	.00314	.00005	.00001
PA3	.00146	.00143	.00350	.00327	.00005	.00001
PB1	.04370	.04776	.06780	.06350	.00138	.00051
PB2	.00405	.00559	.00843	.00784	.00025	.00015
PB3	.00059	.00076	.00077	.00081	.00003	.00003

*Net thickness is less than the gross interval isolated by each zone and is based on radioactive shale thickness from well logs.

- The results of fracture permeability and porosity obtained from the pulse test analysis were consistent with values from semilog and type curve analysis (see Table 5). The bottom zones in each well, which showed good production, exhibited strong pulse test responses. Response in the upper zones was less pronounced due to less fracturing, with wellbore storage dominating the response.

- In the analysis of directional properties, the best ratio of k_{max}/k_{min} was found to be 8.3. The angle of maximum permeability was estimated to be 1.5^{o} above the axis which connects the control well with 10056A. The minimum permeability axis is perpendicular to this axis. These results are presented graphically in Figure 73.

- From the analysis of drainage radius and volume, the drainage radius was found to be approximately 1,300 feet and the drainage volume approximately 8.2×10^{6} cu.ft. These are average values. From the valid range of ω, the drainage radius ranged from 925 to 2,926 feet, and the drainage volume ranged from 4.2×10^{6} to 4.2×10^{7} cu.ft.

- Numerical simulation using Devonian shale models provided estimates of reservoir parameters by history matching the drawdown and buildup interference data in zones PA1 and PB1. Table 10, which follows, summarizes values obtained from the history matching, assuming pseudo-steady-state flow in cylindrical shale matrix elements. The ranges given include all values that give reasonable matches based on all runs made. Mean fracture permeabilities range from .044 md to .089 md based on a thickness of 58 feet, in reasonable agreement with the values calculated from semilog and type curve analysis.

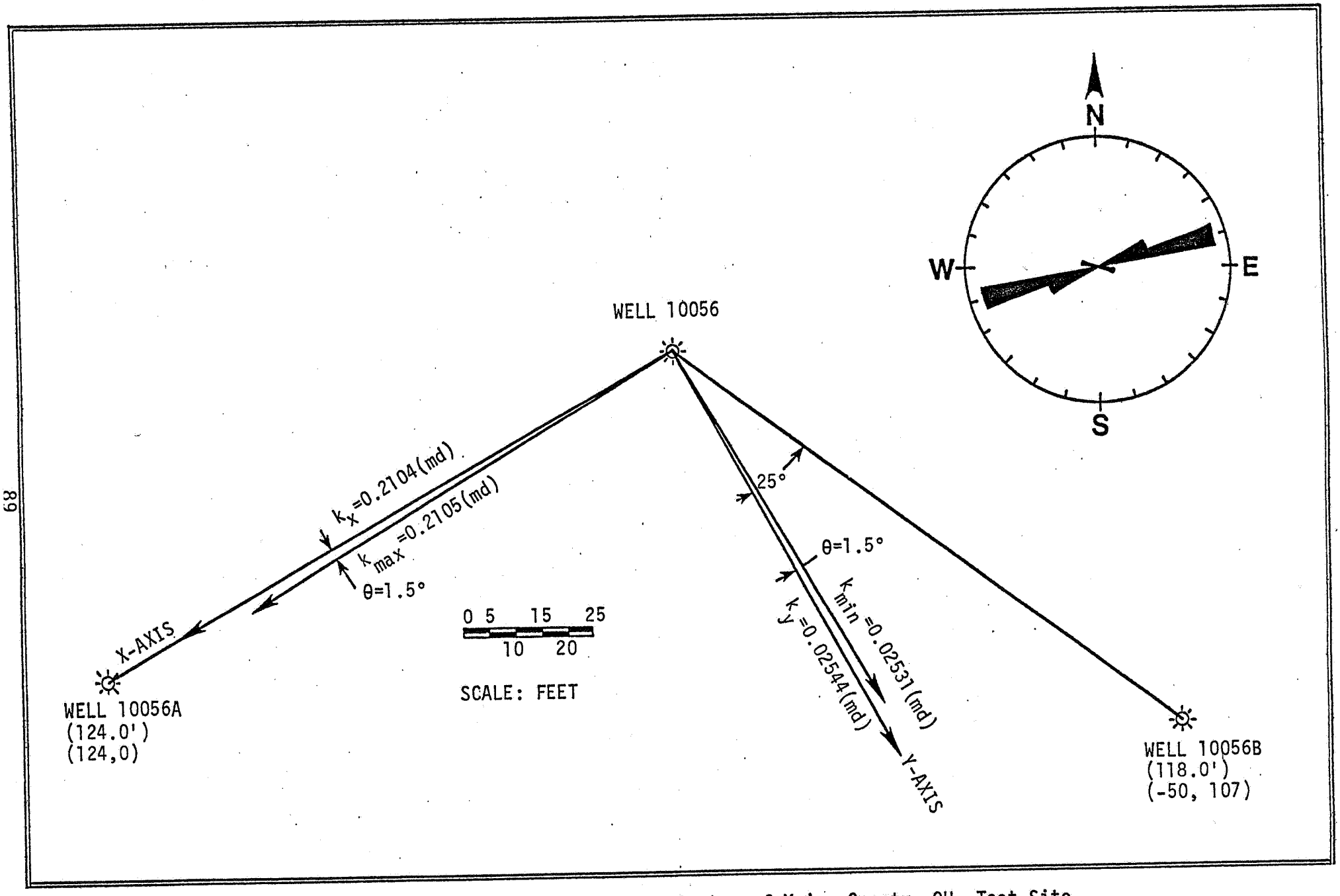

Figure 73: Permeability Anisotropy System of Meigs County, OH, Test Site

Table 10: Reservoir Parameters by History Matching

Parameter	Unit	Value or Range Giving Approximate Match to Interference Data at Wells 10056A and 10056B
ϕ_f	Fraction	.0004 to .0008
k_{fx}	md	.20 to .40
k_{fy}	md	.01 to .02
k_m/a^2	md/ft^2	1×10^{-9} to 25×10^{-9}

- Matrix permeability (based on cores from Well 10056A) has been difficult to determine in the laboratory. Battelle [28] has reported values from <.0002 μd to 1.75 μd, while results from Core Labs indicate that shale matrix permeability is less than .01 μd.

- Three distinct zones were identified. These zones have production/flow characteristics independent of each other and each zone may be considered as a separate layer. This layered system concept will have a significant effect on planning stimulation of Devonian shales.

- Identification of a layered reservoir with directional properties, along with the unconventional gas storage/release mechanism, should impact future development of eastern Devonian shale, since these properties of the reservoir are key parameters required for optimum well spacing and effective stimulation treatments.

5.0

APPLICATION OF RESULTS TO DEVONIAN SHALE RESERVOIR DEVELOPMENT

5.0 APPLICATION OF RESULTS TO DEVONIAN SHALE RESERVOIR DEVELOPMENT

A series of two-dimensional simulation runs was made to investigate the effects of permeability anisotropy and drainage shape on production rate and drainage efficiency. The same parameters used in history matching were applied, except for reservoir size, the ratio of permeability anisotropy, and adsorbed gas content. The objectives of this study were to determine the effect of permeability anisotropy and reservoir shape on economic development in the vicinity of the offset well site. The ratio of k_{max}/k_{min} (R) was varied from 5 to 20, compared to the base value of 10 obtained from analytical results. Since the intent was to determine the effect of permeability anisotropy, gas desorption was not included.

The first part of the study focused on the effect of the permeability ratio on production rate and flow pattern for a large reservoir to minimize boundary effects. The shape of the boundary was square with each side 4250 feet, giving a drainage area of 415 acres. The resultant cumulative production and production rate indicated that the variation of permeability ratio does not significantly affect production in a square drainage area, provided the mean permeability ($k = \sqrt{k_{max}k_{min}}$) is constant. After approximately thirty years of production, there is less than 5 percent difference in cumulative production for R = 5 and R = 20. This is as expected, since boundary effects were marginal.

There are, however, significant differences in the flow patterns. Figure 74 shows the pressure contours at 15 years (5,000 days) and 30 years (11,000 days) of production for R = 5, 10, and 20. The initial pressure used was 690 psi, the initial rock pressure at the Meigs County test site. The elliptical shape of the iso-pressure contours is the result of different degrees of anisotropy. It should be noted that the shape has been approximated near the boundaries due to the size of the finite-difference grid-blocks.

Iso-pressure contours such as those shown in Figure 74 can be helpful in reservoir development. Since new wells should be drilled in the higher-pressure regions, a rectangular drainage pattern is indicated. That is, well spacing should be less in the direction of minimum permeability and greater in the direction of maximum permeability in order to effect optimum reservoir drainage.

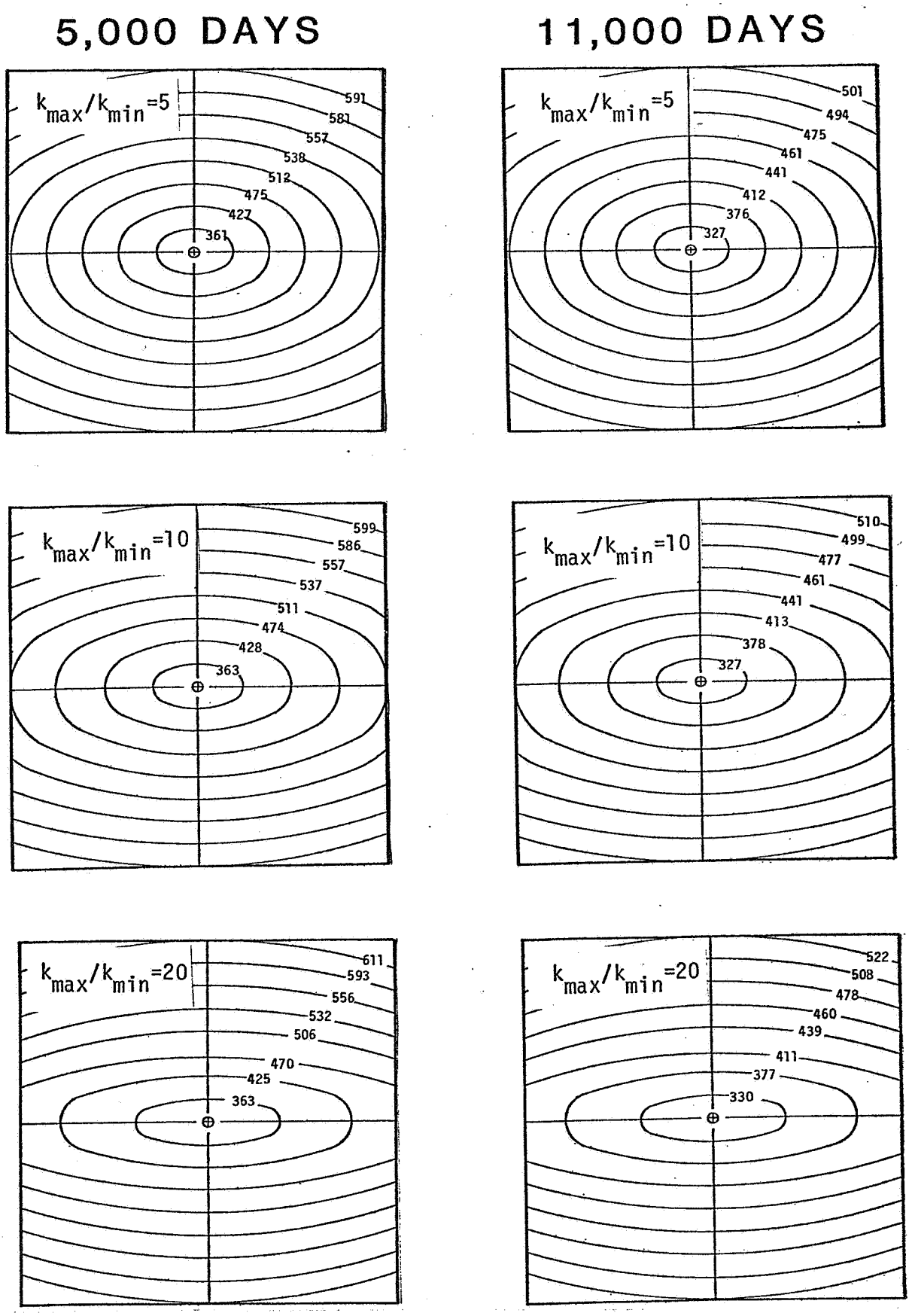

Figure 74: Iso-Pressure Contours in the Meigs County, OH, Reservoir After 5,000 Days and 11,000 Days of Production

The shape of the drainage area can affect production rate and cumulative production for a given anisotropy ratio. For example, with the permeability ratio fixed at $k_x/k_y = 20$, changing the shape of the reservoir boundary from square to rectangular with $\ell x/\ell y = 5$, as shown in Figure 75 results in increased cumulative production of about 7 percent in 10 years. For any given anisotropy ratio, matrix permeability, and drainage size, there will be an optimum drainage shape which can readily be obtained using the simulator.

These results show that a knowledge of permeability anisotropy is important in order to properly space wells. For example, given a large reservoir and a known permeability anisotropy ratio and direction, there will be a certain rectangular drainage area which will recover a desired percentage of the gas-in-place within a given time. More specifically, if a 2-mile-square (2560 acres) Devonian shale reservoir is to be developed on a nominal 80-acre spacing, and the permeability anisotropy is known to be 10 or 20, instead of one well per 80-acre square, wells would be drilled on 80-acre rectangles aligned with the direction of maximum permeability, with a length-to-width ratio determined by simulation.

A direct application to an existing field would be to study the permeability, anisotropy ratio and direction, and shale matrix properties. The potential for infill drilling would then be indicated by high pressure areas within the field.

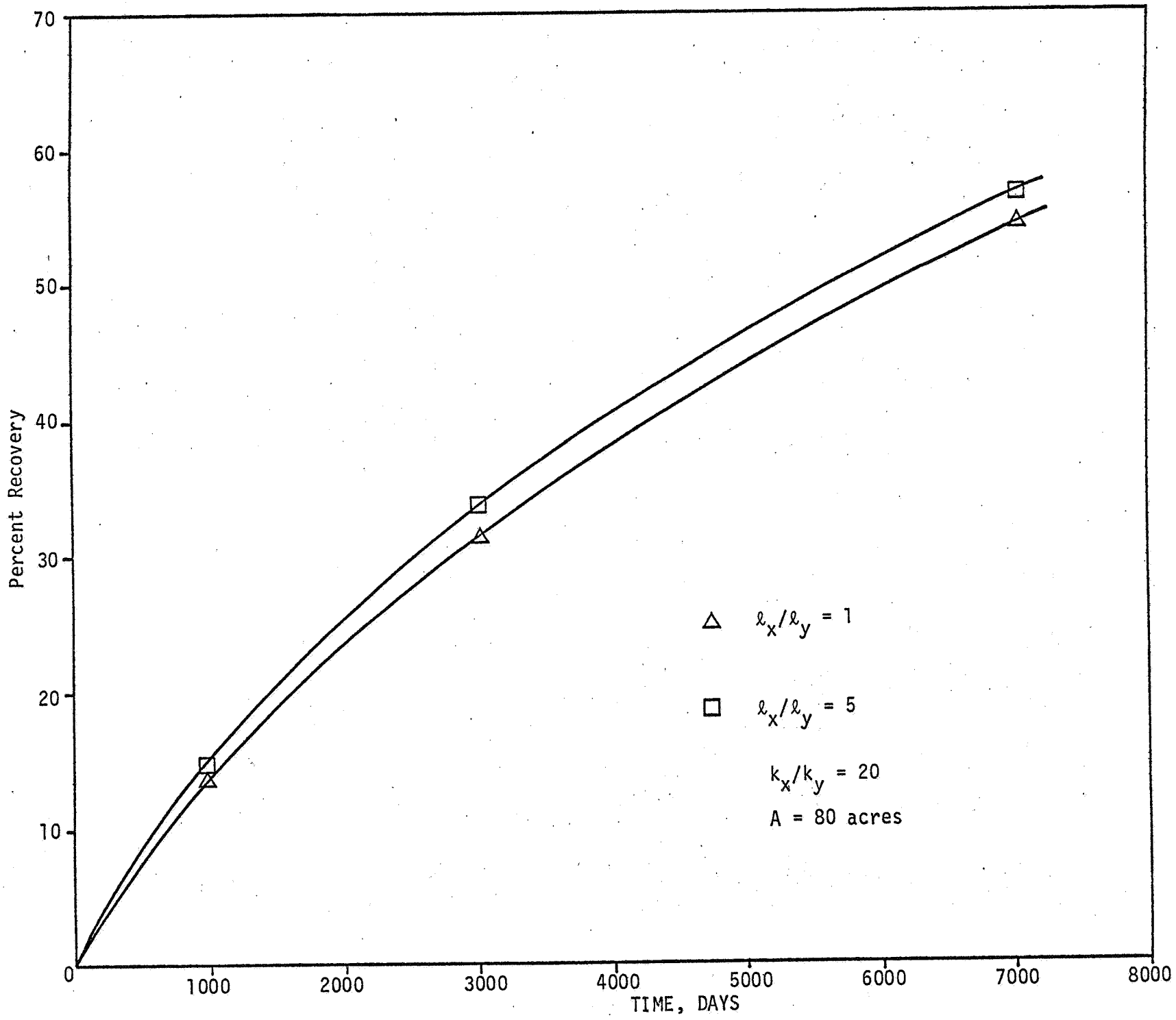

Figure 75: Effect of Drainage Shape on Recovery Efficiency

7.0

APPENDIX

SAI - STEAMBOAT		
Can #	Depth/Ft.	Core Length/Ft.
1	2921.50' → 2921.85'	→ .35'
2	2925.86' → 2926.29'	→ .43'
4	2972.92' → 2973.24'	→ .32'
6	2959.53' → 2959.86'	→ .33'
8	2986.02' → 2986.43'	→ .41'
12	3018.36' → 3018.77'	→ .41'
14	3036.42' → 3036.95'	→ .53'
15	3042.25' → 3042.60'	→ .35'
17	3052.38' → 3052.93'	→ .55'
19	3065.17' → 3065.51	→ .34'
21	3075.41' → 3075.76'	→ .35'
23	3091.25' → 3091.65'	→ .40'
24	3094.23' → 3094.68'	→ .45'
30	3134.54' → 3134.95'	→ .41'
31	3135.19' → 3135.71'	→ .52'
33	3153.29' → 3153.83'	→ .54'
35	3154.53' → 3154.95'	→ .42'
36	3156.23' → 3156.75'	→ .42'
37	3162.28' → 3162.78'	→ .50'
39	3170.42' → 3170.79'	→ .37'
41	3186.22' → 3186.74'	→ .52'
42	3192.08' → 3192.50'	→ .42'
44	3198.48' → 3198.88'	→ .40'
46	3208.55' → 3208.92'	→ .37'
49	3231.41' → 3231.77'	→ .36'
53	3263.50' → 3263.93'	→ .43'
56	3276.60' → 3277.15'	→ .55'
57	3275.60' → 3275.89'	→ .29'
60	3286.38' → 3286.88'	→ .50'
63	3313.33' → 3313.71'	→ .38'
65	3327.03' → 3327.45'	→ .42'
69	3342.16' → 3342.47'	→ .31'

TUBE 1 - 3348.59 - 3354.88
TUBE 2 - 3354.88 - 3355.61
TUBE 3 - 3356.71 - 3362.81
TUBE 4 - 3363.85 - 3372.09

40 Samples - CORE LABS.
32 Samples - SAI - STEAMBOAT
41 Samples - OFFGASSING/BATTELLE

CORE LABS		
Can No.	Depth/Ft.	Core Length/Ft.
3	2930.77' → 2931.33'	→ .56'
5	2960.60' → 2961.07'	→ .47'
7	2976.38' → 2976.79'	→ .41'
9	2990.43' → 2990.85'	→ .42'
10	3003.50' → 3003.97'	→ .47'
11	3017.06' → 3017.60'	→ .54'
13	3033.04' → 3033.49'	→ .45'
16	3051.05' → 3051.49'	→ .44'
18	3056.33' → 3056.87'	→ .54'
20	3072.02' → 3072.52'	→ .50'
22	3085.15' → 3085.62'	→ .47'
25	3099.11' → 3099.63'	→ .52'
26	3104.52' → 3105.04'	→ .52'
27	3115.37' → 3115.84'	→ .47'
28	3120.48' → 3120.88'	→ .40'
29	3127.19' → 3127.76'	→ .57'
32	3147.06' → 3147.47'	→ .41'
34	3154.05' → 3154.53'	→ .48'
38	3165.18' → 3165.69'	→ .51'
40	3181.06' → 3181.49'	→ .43'
43	3195.30' → 3195.80'	→ .50'
45	3205.12' → 3205.69'	→ .57'
47	3210.45' → 3210.88'	→ .43'
48	3215.12' → 3215.56'	→ .44'
50	3234.10' → 3234.64'	→ .54'
51	3250.09' → 3250.52'	→ .43'
52	3251.22' → 3251.65'	→ .43'
54	3269.21' → 3269.66'	→ .45'
55	3270.07' → 3270.52'	→ .45'
58	3278.37' → 3278.70'	→ .33'
59	3281.06' → 3281.61'	→ .55'
61	3302.10' → 3302.50'	→ .40'
62	3310.18' → 3310.73'	→ .55'
64	3328.50' → 3328.99'	→ .49'
66	3327.45' → 3327.93'	→ .48'
67	3337.11' → 3337.57'	→ .46'
68	3338.19' → 3338.67'	→ .48'
70	3352.46' → 3353.00'	→ .54'
71	3355.18' → 3355.64'	→ .46'
72	3367.51' → 3367.96'	→ .45'

OFFGASSING/BATTELLE		
Can No.	Depth/Ft.	Core Length/Ft.
0-1	2933.92' → 2934.30'	→ .39'
0-2	2940.02' → 2940.50'	→ .48'
0-3	2956.36' → 2956.81'	→ .45'
0-4	2973.24' → 2973.70	→ .46'
0-5	2980.88' → 2981.35'	→ .47'
0-6	3002.01' → 3002.42'	→ .41'
0-7	3016.61' → 3017.06'	→ .45'
0-8	3025.92' → 3026.36'	→ .44'
0-9	3033.54' → 3033.96'	→ .42'
0-10	3050.02' → 3050.47'	→ .45'
0-11	3061.55' → 3061.99'	→ .44'
0-12	3084.06' → 3084.54'	→ .48'
0-13	3095.23' → 3095.67'	→ .44'
0-14	3105.13' → 3105.58'	→ .45'
0-15	3113.28' → 3113.74'	→ .46'
0-16	3121.30' → 3121.71'	→ .41'
0-17	3128.08' → 3128.55'	→ .47'
0-18	3146.41' → 3146.89'	→ .48'
0-19	3152.09' → 3152.57'	→ .48'
0-20	3166.41' → 3166.87'	→ .46'
0-21	3180.12' → 3180.55'	→ .43'
0-22	3199.41' → 3199.87'	→ .46'
0-23	3208.06' → 3208.52'	→ .46'
0-24	3217.11' → 3217.56'	→ .45'
0-25	3193.38' → 3193.81'	→ .43'
0-26	3230.47' → 3230.90'	→ .43'
0-27	3240.40' → 3240.85'	→ .45'
0-28	3250.51' → 3250.98'	→ .47'
0-29	3267.05' → 3267.44'	→ .39'
0-30	3276.50' → 3276.89'	→ .39'
0-31	3273.52' → 3273.91'	→ .47'
0-32	3287.40' → 3287.84'	→ .44'
0-41	3289.06' → 3289.85'	→ .79'
0-33	3295.99' → 3296.47'	→ .48'
0-42	3300.28' → 3300.98'	→ .70'
0-34	3308.60' → 3309.00'	→ .40'
0-35	3314.49' → 3314.95'	→ .46'
0-36	3325.20' → 3325.66'	→ .46'
0-37	3341.40' → 3341.87'	→ .47'
0-38	3343.67' → 3344.14'	→ .47'
0-39	3358.21' → 3358.64'	→ .43'
0-40	3369.48' → 3369.95'	→ .47'

Core Sample Distribution, Offset Well Test Program, Meigs County, OH

MEIG'S COUNTY SHALE DATA SUMMARY
(continued)

Sample No.	Permeability		Physical Properties					Flow Simulation			Compressibility Factor[c]	
	P_c, Psig	Perm, μd @P=250 psi	Bulk Density g/cc	Porosity, percentage	Surface Area, m^2/g	Average[a] Pore Radius, Å	Kerogen, wt. percentage	Sample Length, cm	V_{CH_4} (P=500÷200) cc-atm Total	Shale	Number 1.	Number 2.
22	3199	52.6			10.4		<0.1	5.47	2653	1050		
23	3208	0.010	2.627	1.87	4.5	32	<0.1		(e)			5.3×10^{-3}
24	3217	0.18	2.562	6.67	9.3	56	<0.1	3.83	2400	700	8.7×10^{-3}	5.2×10^{-3}
25	3193	10.0	2.646	4.99	8.6	44	<0.1		(e)			9×10^{-4}
26	- -	b	2.657	2.67	4.9	41	<0.1		(e)			
27	3240	0.12±0.09	2.628	--	4.0	--	<0.1		(e)			- -
28	- -	(b)	2.669	3.03	8.4	27	<0.1		(e)			
29	3267	0.43±0.07	2.612	3.15	3.3	73	<0.1		(e)			4.7×10^{-3}
30	3276	0.015	2.660	--	3.3	--	0.73		(e)			- -
31	3274	0.024	2.579	--	5.2	--	<0.1					- -
32	3288	0.14	2.514	1.07	4.4	19	<0.1	12.49	2161	287	(-2×10^{-3})	3.8×10^{-3}
33	3296	0.026	2.480	5.16	4.9	85	<0.1		(e)			5.2×10^{-3}
34	3308	5.36±0.27	2.719	0.772	7.2	8	<0.1	9.73	2218	350	(-7×10^{-2})	(-3.0×10^{-2})
35	3238	0.12±0.01	2.684	2.72	5.6	36	<0.1	11.77	2248	282	2×10^{-3}	4.9×10^{-3}
36	3325	~0.004	2.678	0.896	6.2	11	<0.1		(e)			5.0×10^{-3}
37	3341	28.2	2.769	2.02	6.5	22	1.10	3.98	2782	1262	(-3×10^{-2})	(-1.9×10^{-3})
38	3334	0.098	2.527	2.26	3.1	58	0.19		(e)			4.9×10^{-3}
39	3358	29.7	2.522	2.26	3.3	54	0.40	12.38	2748	755	3.5×10^{-3}	(-6×10^{-3})
40	3369	~0.004	2.503	0.320	2.1	12	1.30		(e)			4.7×10^{-3}
41	3289	<0.004	2.497	8.15	4.45	147	1.40		(d)			- -
42	3300	<0.004	2.422	4.21	4.3	81	(d)		(d)			- -

a. Cylindrical pore basis.
b. Taken from consistent portions of data in Appendix A.
c. Estimated using equation 9; 1 = simulation data used; 2 = permeability data.
d. Flow rate too small, perm <0.02 μd.
e. Sample broken, no useable fragments.
f. Sample not received.
g. Omitted per sponsor's instructions.

BATTELLE LABORATORIES DATA
Core Analysis

MEIG'S COUNTY SHALE DATA SUMMARY

Sample No.	Permeability		Physical Properties					Flow Simulation			Compressibility Factor[c]	
	P_c, Psig	Perm, μd @P=250 psi	Bulk Density g/cc	Porosity, percentage	Surface Area, m^2/g	Average[a] Pore Radius, Å	Kerogen, wt. percentage	Sample Length, cm	V_{CH_4} (P=500→200) cc-atm Total	V_{CH_4} (P=500→200) cc-atm Shale	Number 1.	Number 2.
1	- -	g	2.616	4.55	6.9	50	g		(d)			
2	- -	g	2.685	5.55	9.7	43	g		(e)			
3	2957	0.064±.002	2.658	3.16	8.3	29	g	3.96	2728	1200	7.6×10^{-3}	5.6×10^{-3}
4	- -	g	g	g	g	- -	g		(d)			
5	2981	117±19	2.605	6.07	4.3	108	g		(e)			(-2.8×10^{-3})
6	- -	g	2.728	7.55	8.0	69	g		(d)			
7	3016	42	2.489	6.11	4.8	102	g		(e)			7.8×10^{-4}
8	2965	1.6	2.663	3.08	5.7	41	g	11.90	2285	536	3.7×10^{-3}	3.7×10^{-3}
9	2915	0.19	2.555	0.94	4.6	16	<0.1					3.5×10^{-3}
10	- -	g	2.524	2.81	5.1	44	<0.1		(e)			
11	- -	g	2.650	4.97	6.3	60	<0.1	5.97	836	(~854)		
12	- -	g	g	g	g	- -	(f)		(f)			
13	- -	g	g	g	10.4	- -	0.2	5.47	2188	700		
14	- -	g	g	g	7.8	- -	0.2		(e)			
15	- -	g	g	g	7.9	- -	0.1		(d)			
16	- -	g	g	g	7.2	- -	0.1	5.00	1500	390		
17	- -	g	g	g	5.7	- -	<0.1		(e)			
18	3146	~0.004	2.532	2.61	7.6	27	0.2	13.43	1853	0		5.5×10^{-3}
19	- -	g	2.465	2.76	5.0	45	<0.1		(d)			
20	3166	0.16	2.692	6.50	11.3	43	<0.1		(e)			5.2×10^{-3}
21	3166	16.9	2.671	3.71	10.1	28	<0.1	6.99	2544	531		(-5.3×10^{-3})

BATTELLE LABORATORIES DATA
Core Analysis

Special Core Analysis Study

for

SCIENCE APPLICATIONS, INC.

No. 10056A Well
Devonian Shale Formation
Meigs County, Ohio

7501 STEMMONS FREEWAY, BOX 47547, DALLAS, TEXAS 75247 · 214/631-8270

CORE LABORATORIES, INC.
Special Core Analysis

January 13, 1982

Science Applications, Inc.
Suite 8
Chestnut Ridge Professional Bldg.
Chestnut Ridge Road
Morgantown, West Virginia 26505

Attention: Javaid Alam

Subject: Special Core Analysis Study
Offset Well No. 10056A
Devonian Shale
Meigs County, Ohio
File Number: SCAL-308-81061

Gentlemen:

In response to a proposal issued on January 13, 1981, signed by Core Laboratories, Inc., Area Manager John M. Dacy, Science Applications, Inc., representative Yvonne L. Forrest authorized, in Purchase Order Number 15-820011-56, dated August 17, 1981, the Special Core Analysis Department of Core Laboratories, Inc., at Dallas, Texas, to perform Klinkenberg Permeability (under confining stress) and Porosity Determinations on well core material from the subject well. This is a final report on the results of this study and contains data previously reported in preliminary form on November 19, 1981.

Sample Preparation

Forty sealed metal cans containing one well core segment each were received at Core Laboratories, Inc., on March 3, 1981. These segments represented various depth intervals ranging from approximately 2930 feet to approximately 3370 feet of the subject well.

Using orientation diagrams provided by Science Applications, Inc., two 1-inch diameter, cylindrical, horizontally oriented core plug samples were drilled from each frozen well core segment using a diamond core drill with liquid nitrogen as the bit coolant and lubricant. It should be noted that numerous samples were unobtainable due to fractures along bedding planes. All core plugs were kept frozen until tested, and the whole core remnants were represerved by wrapping them in Saran and aluminum foil, and then dipping them in a strippable plastic. The core

plugs used in this study are lithologically described and identified as to sample number and depth interval on Pages 1 and 2 of this report.

Klinkenberg Permeability (under confining stress) and Porosity

Attempts were made to determine Klinkenberg permeability on three core plugs (71A, 72A, 72B) using a steady-state technique. While still frozen, each core plug was measured for bulk volume (by calipered length times area and by mercury pycnometer) and then loaded in a hydrostatic core holder. A confining stress of approximately 840 psig was applied, and each core plug was allowed to come to stress equilibrium and thaw overnight. Over a period of several days, attempts were made to achieve a steady-state measureable flow rate of nitrogen through each core plug using 3 to 8 different upstream pressures ranging from 1 to 50 psig. Unfortunately, a constant rate of flow could not be achieved using current steady-state laboratory techniques due to the ultra-low permeabilities of the core plugs. As a result, all testing was suspended until the testing program could be reevaluated.

In a telephone conversation on September 18, 1981, Javaid Alam authorized, after reevaluating the test program, the use of a non-steady state ultra-low permeability determination technique available from the Research and Development Department of Core Laboratories, Inc. First, the Boyle's Law porosity of each thawed core plug was determined using a small volume extended range porosimeter with helium as the gaseous medium. The Klinkenberg permeability of each core plug was then determined (using methane as the gaseous medium) under a confining stress of 1000 psig and a flow rate of 100 psi. A detailed explanation of the procedures and equipment used to acquire these determinations is presented in the enclosed article (SPE 10075) authored by members of the Core Laboratories, Inc., Research and Development staff. The results of the Klinkenberg permeability (under confining stress) and porosity determinations are presented on Pages 3 and 4. Samples 32A and 43B failed during testing due to vertical fractures.

It has been a pleasure performing this study on behalf of Science Applications, Inc. Should there be any questions concerning these test results, or if we may be of any further assistance, please do not hesitate to contact us.

Very truly yours,

Core Laboratories, Inc.

John A. Koerner

John A. Koerner, Laboratory Supervisor
Special Core Analysis

JAK:DLM:sd
10 cc. - Addressee with enclosure

IDENTIFICATION AND LITHOLOGICAL DESCRIPTION OF SAMPLES

Science Applications, Inc.
No. 10056A Well

Devonian Shale Formation
Meigs County, Ohio

Sample Identification	Depth, feet	Lithological Description
3B	2930.77-31.33	Sh, lt gry, v/well indurated, lam, pyr
10B	3003.5- 03.97	Sh, gry-brn, v/well indurated, lam
11A	3017.06-17.60	Sh, dk gry, v/well indurated, lam
16B	3051.05-51.49	Sh, dk gry, v/well indurated, lam
18A	3056.33-56.87	Sh, dk gry, v/well indurated
18B	3056.33-56.87	Sh, dk gry, v/well indurated
20A	3072.02-72.52	Sh, dk gry, v/well indurated
25A	3099.11-99.63	Sh, dk gry, v/well indurated
25B	3099.11-99.63	Sh, dk gry, v/well indurated
26A	3104.52-05.04	Sh, dk gry, v/well indurated, tr pyr
27B	3115.37-15.84	Sh, lt gry, v/well indurated, tr pyr
29B	3127.19-27.76	Sh, lt gry, v/well indurated, tr pyr
32A	3147.06-47.47	Sh, lt gry, v/well indurated, pyr
32B	3147.06-47.47	Sh, lt gry, v/well indurated, pyr
34B	3154.05-54.53	Sh, lt gry, v/well indurated, pyr
38B	3165.18-65.69	Sh, lt gry, v/well indurated, pyr
43A	3195.3 -95.8	Sh, dk gry, v/well indurated
43B	3195.3 -95.8	Sh, dk gry, v/well indurated
45A	3205.12-05.69	Sh, dk gry, v/well indurated, conch fracs
46A	3208.55-08.92	Sh, dk gry, v/well indurated
47B	3210.45-10.88	Sh, dk gry, v/well indurated
48B	3215.12-15.56	Sltst, lt gry, v/well indurated, s/calc, lam, pyr
50A	3234.10-34.64	Sh, dk gry, v/well indurated

This report, based on observations and materials supplied by the client, is prepared for the exclusive and confidential use by the client. The analyses, opinions, or interpretations contained herein represent the judgement of Core Laboratories, Inc.; however, Core Laboratories, Inc., and its employees assume no responsibility and make no warranties or representations as to the utility of this report to the client or as to the productivity, proper

IDENTIFICATION AND LITHOLOGICAL DESCRIPTION OF SAMPLES

Science Applications, Inc.
No. 10056A Well

Devonian Shale Formation
Meigs County, Ohio

Sample Identification	Depth, feet	Lithological Description
54A	3269.21-69.66	Sh, dk gry, v/well indurated
54B	3269.21-69.66	Sh, dk gry, v/well indurated, lam, v/argil
55A	3270.07-70.52	Sh, dk gry, v/well indurated, lam
55B	3270.07-70.52	Sh, dk gry, v/well indurated, lam
58A	3278.37-78.70	Sltst, dk gry, v/well indurated, v/fn gr, gd srt, sh lam, v/argil
58B	3278.37-78.70	Sltst, dk gry, v/well indurated, v/fn gr, gd srt, sh lam, v/argil
59A	3281.06-81.61	Sh, gry-brn, v/well indurated
61B	3302.10-02.50	Sh, gry, v/well indurated, lam
62B	3310.18-10.73	Sh, dk gry, v/well indurated, v/argil
66A	3327.45-27.93	Sltst, lt gry, v/well indurated, v/fn gr, incl, pyr, calc, frac
66B	3327.45-27.93	Sltst, lt gry, v/well indurated, v/fn gr, pyr, calc, frac
67A	3337.11-37.57	Sh, lt gry, v/well indurated, pyr, v/argil
68A	3338.19-38.67	Sh, lt gry, v/well indurated s/calc, pyr, v/argil
68B	3338.19-38.67	Sh, lt gry, v/well indurated s/calc, pyr, v/argil
70A	3352.46-53.00	Sh, lt gry, v/well indurated, incl, v/argil
70B	3352.46-53.00	Sh, lt gry, v/well indurated incl, v/argil
71A	3355.18-55.64	Sh, gry, v/well indurated
71B	3355.18-55.64	Sh, gry, v/well indurated
72A	3367.51-67.96	Sh, dk gry, v/well indurated
72B	3367.51-67.96	Sh, dk gry, v/well indurated

This report, based on observations and materials supplied by the client, is prepared for the exclusive and confidential use by the client. The analyses, opinions, or interpretations contained herein represent the judgement of Core Laboratories, Inc.; however, Core Laboratories, Inc., and its employees assume no responsibility and make no warranties or representations as to the utility of this report to the client or as to the productivity, proper

CORE LABORATORIES, INC.

Special Core Analysis

File SCAL-308-81061

PERMEABILITY TO METHANE AND HELIUM POROSITY

Science Application, Inc.
No. 10056A Well

Devonian Shale Formation
Meigs County, Ohio

Sample Identification	Depth, feet	Permeability to Methane, millidarcys	Porosity, percent	Overburden Pressure psig
3B	2930.77-2931.33	0.0020	1.3	1000
10B	3003.5 -3003.97	<0.00001	1.2	1000
11A	3017.06-3017.6	<0.00001	1.2	1000
16B	3051.05-3051.49	0.0001	1.4	1000
18A	3056.33-3056.87	<0.00001	1.6	1000
18B	3056.33-3056.87	<0.00001	1.3	1000
20A	3072.03-3072.52	0.0007	1.4	1000
25A	3099.11-3099.63	0.0355	2.2	1000
25B	3099.11-3099.63	<0.00001	1.7	1000
26A	3104.52-3105.04	0.0002	1.2	1000
27B	3115.37-3115.84	0.0520	1.4	1000
29B	3127.19-3127.76	0.0018	1.0	1000
32A	3147.06-3147.47	Failed	1.3	1000
32B	3147.06-3147.47	0.0262	1.2	1000
34B	3154.05-3154.53	<0.00001	0.8	1000
38B	3165.18-3165.69	0.0001	1.0	1000
43A	3195.3-3195.8	Failed	0.2	1000
43B	3195.3-3195.8	0.0036	1.2	1000
45A	3205.12-3205.69	0.0002	1.2	1000
46A	3208.55-3208.92	0.0056	2.7	1000
47B	3210.45-3210.88	<0.00001	1.0	1000
48B	3215.12-3215.56	<0.00001	0.9	1000
50A	3234.10-3234.64	<0.00001	1.2	1000
54A	3269.21-3269.66	<0.00001	1.0	1000
54B	3269.21-3269.66	<0.00001	1.3	1000
55A	3270.07-3270.52	<0.00001	0.9	1000
55B	3270.07-3270.52	<0.00001	1.0	1000
58A	3278.37-3278.70	<0.00001	1.0	1000
58B	3278.37-3278.70	<0.00001	1.3	1000
59A	3281.06-3281.61	<0.00001	1.6	1000
61B	3302.10-3302.50	<0.00001	0.8	1000
62B	3310.18-3310.73	0.00006	1.2	1000
66A	3327.45-3327.93	0.00008	1.1	1000
66B	3327.45-3327.93	0.0091	1.1	1000
67A	3337.11-3337.57	0.0011	1.0	1000
68A	3338.19-3838.67	<0.00001	1.1	1000
68B	3338.19-3338.67	<0.00001	0.7	1000

This report, based on observations and materials supplied by the client, is prepared for the exclusive and confidential use by the client. The analyses, opinions, or interpretations contained herein represent the judgement of Core Laboratories, Inc.; however, Core Laboratories, Inc., and its employees assume no responsibility and make no warranties or representations as to the utility of this report to the client or as to the productivity, proper

CORE LABORATORIES, INC.

Special Core Analysis

File SCAL-308-81061

PERMEABILITY TO METHANE AND HELIUM POROSITY

Science Application, Inc.
No. 10056A Well

Devonian Shale Formation
Meigs County, Ohio

Sample Identification	Depth, feet	Permeability to Methane millidarcys	Porosity, percent	Overburden Pressure psig
70A	3352.46-3353.0	<0.00001	0.9	1000
70B	3352.46-3353.0	<0.00001	1.0	1000
71B	3355.18-3355.64	<0.00001	1.0	1000
71A	3355.18-3355.64	<0.00001	1.1	1000
72A	3367.51-3367.96	<0.00001	1.0	1000
72B	3367.51-3367.96	<0.00001	0.9	1000

This report, based on observations and materials supplied by the client, is prepared for the exclusive and confidential use by the client. The analyses, opinions, or interpretations contained herein represent the judgement of Core Laboratories, Inc.; however, Core Laboratories, Inc., and its employees assume no responsibility and make no warranties or representations as to the utility of this report to the client or as to the productivity, proper

8.0

REFERENCES

8.0 REFERENCES

1. Mavor, M. J., and Cinco, Ley, H.: "Transient Pressure Behavior of Naturally Fracture Reservoirs", SPE 7977, presented at SPE 1979 California Regional Meeting, April 18-20, 1979.

2. Agarwal, R.G., Al-Hussainy, R., and Ramey, H. J., Jr.: "An Investigation of Wellbore Storage and Skin Effect in Unsteady Liquid Flow: I. Analytical Treatment," Soc. Pet. Eng. J. (Sept. 1970), p. 279.

3. Crawford, G. E., Hagedorn, A. R., and Pierce, A. E.: "Analysis of Pressure Buildup Tests in a Naturally Fractured Reservoir," J. Pet. Tech. (Nov. 1976), pp. 1295-1300.

4. de Swann, O. A.: "Analytic Solutions for Determining Naturally Fractured Reservoir Properties by Well Testing," Soc. Pet. Eng. J. (June 1976), pp. 117-122.

5. Kazemi, H.: "Pressure Transient Analysis of Naturally Fractured Reservoirs with Uniform Fracture Distributions," Trans. AIME (1969), 246, pp. 451-642.

6. Muskat, M.: "The Flow of Homogeneous Fluids Through Porous Media, J. W. Edwards, Inc., Ann Arbor, Mich. (1946) 621.

7. Najurieta, H. L.: "A Theory for the Pressure Transient Analysis in Naturally Fractured Reservoirs," SPE Paper 6017, Presented at the 51st Technical Conference of the SPE, New Orleans, LA, Oct. 3-6, 1976.

8. Odeh, A. S.: "Unsteady-State Behavior of Naturally Fractured Reservoirs," Soc. Pet. Eng. J. (March 1961) pp. 60-64.

9. Ramey, H. J. Jr.: "Short-Time Well Test Data Interpretation in the Presence of Skin Effect and Wellbore Storage," JPT (Jan. 1970), p. 97.

10. Ramey, H. J., Jr.: "Practical Use of Modern Well Test Analysis," SPE Paper 5878, Presented at the 51st Technical Conference of the SPE, New Orleans, LA, Oct. 3-16, 1976.

11. Ramey, H. J., Jr., and Cobb, W. M.: "A General Pressure Buildup Theory for a Well in a Closed Drainage Area," JPT (Dec. 1971), p. 1493.

12. Stehfest, H.: "Algorithm 368, Numerical Inversion of Laplace Transforms," D-5 Communications of the ACM (Jan. 1970), 13, No. 1, pp. 47-49.

13. Streltsova, T. D.: "Hydrodynamics of Groundwater Flow in a Fractured Formation," Water Resources Research Vol 12, No. 13 (June 1976), p. 405.

14. Streltsova-Adams, T. D.: "Well Hydraulics in Heterogeneous Aquifer Formations," Advances in Hydroscience Vol. II., New York: Academic Press, Inc. (1978).

15. Uldrich, David O., and Ershaghi, I.: "A Method for Estimating the Interporosity Flow Parameter in Naturally Fractured Reservoirs," SPE Paper 7142, Presented at the 1978 California Regional Meeting of the SPE-AIME, San Francisco, CA, April 12-14, 1978.

16. Van Everdingen, A. F., and Hurst, W.,: "The Application of the Laplace Transform to Flow Problems in Reservoirs," Trans., AIME (1949) 186, 305-324B.

17. Warren, J. E., and Root, P. J.: "The Behavior of Naturally Fractured Reservoirs," Soc. Pet. Eng. J. (Sept. 1963), pp. 245-255.

18. Warren, J. E., and Root, P. J. L.: "Discussion on Unsteady-State Behavior of Naturally Fractured Reservoirs," Soc. Pet. Eng. J. (Mar. 1965).

19. Raghavan, R., et al., Well Test Analysis for Devonian Shale Wells, Univ. of Tulsa, USDOE Contract No. DE-AC21-80MC14645, Sept. 30, 1981.

20. Chu, W. C., Garcia-Rivera, J., and Raghavan, R.: "Analysis of Interference Test Data Influenced by Wellbore Storage and Skin at the Flowing Well", J. Pet. Tech. (Jan, 1980) 171-178.

21. Prats, M., and Scott, J.B.: "Effects of Wellbore Storage on Pulse Test Pressure Response," J. Pet. Tech. (June 1975) 707-709.

22. Mondragon, J. J., and Menzie, D. E.: "An Empirical Method to Correct Pulse Test Results for Wellbore Storage at the Pulsing Well," SPE 8207 presented at the 54th SPE Annual Meeting, Las Vegas, Nevada, Sept. 23-26, 1979.

23. Kamal, J., and Brigham, W. E., Design and Analysis of Pulse Tests with Unequal Pulse and Shut-in Periods, SPE Reprint 14, Pressure Transient Testing Methods, 1980, pp. 151-158.

24. Papadopulus, I.S.: "Nonsteady Flow to a Well in an Infinite Anisotropic Aquifer", Proc. 1965 Dubrovnik Symposium on Hydrology of Fractured Rocks, Intl. Assoc. of Sci. Hydrology (1965) I, 21-31.

25. Ramey, H. J., Jr.: "Interference Analysis for Anisotropic Formations--A Case History", J. Pet. Tech. (Oct. 1975) 1290-1298.

26. Science Applications, Inc. (SAI) A Reservoir Engineering Study for the Offset Well Test Program, Dec. 13, 1980, prepared under Contract DE-AM21-78MC08216, Task 23.

27. Raghavan, R., Private Communication.

28. Cobb, W. M., and Smith, J.T.: An Investigation of Pressure Buildup Tests in Bounded Reservoirs", J. Pet. Techn., Aug. 1975, 991-996.

29. Ramey, H. J., Jr., Kumar, A., Gulati, M.S." Gas Well Test Analysis Under Water Drive Conditions, Monograph on Project 61-51, AGA, Arlington, VA, 312.

30. SAI, SUGAR User's Manual, July 31, 1981.

31. SAI, SUGAR-MD User's Manual, September 30, 1981.

32. Coutant, R. W.: "Mechanisms of Natural Gas Release from Devonian Shale," Battelle Columbus Laboratories, S.A.I. Task No. 212, July 23, 1981.

33. SAI Final Report for Analysis of Devonian Shale Multi-Well Interference Tests in Meigs County, Ohio, Feb. 23, 1982, prepared under Contract No. DE-AC21-81MC16283.